COLUMBIA UNIVERSITY

DEPARTMENT OF PHYSICS

■ PROGRESS REPORT NO. 11

THIRD QUARTERLY PROGRESS REPORT

JUNE 16, 1965 THROUGH SEPTEMBER 15, 1965

To:

THE JOINT SERVICES TECHNICAL ADVISORY COMMITTEE

REPRESENTING: THE U.S. ARMY ELECTRONICS LABORATORIES
THE U.S. ARMY RESEARCH OFFICE
THE OFFICE OF NAVAL RESEARCH
THE AIR FORCE OFFICE OF SCIENTIFIC RESEARCH

COLUMBIA RADIATION LABORATORY NEW YORK, NEW YORK 10027

■ SEPTEMBER 15, 1965

The research reported in this document was made possible through support extended the Columbia Radiation Laboratory, Columbia University, by the Joint Services Electronics Program (U. S. Army Electronics Laboratories and U. S. Army Research Office, Office of Naval Research, and the Air Force Office of Scientific Research) under Contract DA 28-043 AMC-00099(E).

Portions of this work were also supported by:

U. S. Army Research Office (Durham)

Grants DA-ARO(D)-31-124-G568 and DA-ARO-D-31-124-G699 and Contracts DA-31-124-ARO-D-224, DA-31-124-ARO-D-305, DA-31-124-ARO-D-341 and AD-31-124-ARO-D-296

National Science Foundation

Grants NSF-GP 1031, NSF-GP 3385, NSF-GP 4324 and NSF-GP 3379

Air Force Office of Scientific Research

Grant AF-AFOSR-330-63

Office of Naval Research

Contracts Nonr-266(45), Nonr-3994(00), and Nonr-4259(10)

National Aeronautics and Space Administration

Grants NsG-360 and NsG-442

The support of these agencies is acknowledged in footnotes in the text.

COLUMBIA RADIATION LABORATORY

RESEARCH INVESTIGATION DIRECTED TOWARD EXTENDING THE USEFUL RANGE OF THE ELECTROMAGNETIC SPECTRUM

Progress Report No. 11

Third Quarterly Progress Report

June 16, 1965 through September 15, 1965

Contract DA 28-043 AMC-00099(E)
(Continuation of Contract DA 36-039 SC-90789)

CU-9-65 AMC-00099(E) Physics

Object of the research:

Physical research in fields in which microwave frequency techniques are employed; the development of microwave electronic and circuit devices.

The research reported in this document was made possible through support extended the Columbia Radiation Laboratory, Columbia University, by the Joint Services Electronics Program (U. S. Army Electronics Laboratories and U. S. Army Research Office, Office of Naval Research, and the Air Force Office of Scientific Research) under Contract DA 28-043 AMC-00099(E).

Prepared by R. Novick

COLUMBIA UNIVERSITY

Division of Government Aided Research

New York, N. Y. 10027

September 15, 1965

TABLE OF CONTENTS

The names of the authors are arranged alphabetically.

PUBLICATIONS AND REPORTS

Publications

M. Hessel and P. Kusch, "Deviation from the $1/r^6$ Potential in the Scattering of a Polar Molecule by Non-Polar Gases," J. Chem. Phys. 43, 305 (1965).

W. Happer and E. B. Saloman, "Observation of Different Lifetimes for Atomic States Excited with Linearly and Circularly Polarized Light," Phys. Rev. Letters 15, 441 (1965).

Isaac L. Bass[1] and Robert Mieher,[2] "ENDOR Study of the Self-Trapped Hole Associated with Lithium in NaF," Phys. Rev. Letters 15, 25 (1965).

Papers by CRL Staff Members Presented at Scientific Meetings

American Physical Society Meetings:

New York, N. Y., June 23-25, 1965.

E. B. Saloman and W. Happer, Jr., "Coherence Narrowing and Collision Broadening in the $(6p7s)^3P_1^o - (6p^2)^3P_{0,1,2}$ Transitions in Lead," Bull. Am. Phys. Soc. 10, 596 (1965).

A. Khadjavi, A. Lurio, and W. Happer, Jr., "Electric-Field Level Crossings in Mercury," Bull. Am. Phys. Soc. 10, 596 (1965).

Y. Yeh, "Laser Studies of Molecular Motion in Liquids," Bull. Am. Phys. Soc. 10, 609 (1965).

R. Marzke and R. L. Mieher, "ENDOR of the V_K Center in CaF_2", Bull. Am. Phys. Soc. 10, 615 (1965).

D. F. Daly and R. L. Mieher, "ENDOR Hyperfine Constants of the V_K Center in LiF and NaF," Bull. Am. Phys. Soc. 10, 615 (1965).

M. L. Dakss and R. L. Mieher, "ENDOR Study of the H Center in LiF," Bull. Am. Phys. Soc. 10, 615 (1965).

---

1. Present Address: Department of Physics, Stanford University, Stanford, California.
2. Present Address: Department of Physics, Purdue University, Lafayette, Indiana.

Honolulu, Hawaii, September 2-5, 1965.

W. Ho, I. Kaufman, and P. Thaddeus, "Microwave Absorption in Models of the Atmosphere of Venus," Bull. Am. Phys. Soc. 10, 705 (1965).

Physics of Quantum Electronics Conference, San Juan, Puerto Rico, June 28-30, 1965.

N. A. Kurnit, I. D. Abella, and S. R. Hartmann, "Photon Echoes in Ruby."

R. Novick, P. Davidovits, W. Happer, Jr., and W. A. Stern, "Light Shift, Light Modulation, and Phase Pulling in the Optically Pumped Rubidium Maser."

S. S. Alpert, R. Novick, L. Seigel, and Y. Yeh, "Observation of Time-Dependent Density Fluctuations in Carbon Dioxide Near the Critical Point Using a He-Ne Laser."

M. Lipeles, R. Novick, and N. Tolk, "Radiation from the Impact of Very Low Energy He^+," Fourth International Conference on Physics of Electronic and Atomic Collisions, L'Université Laval, Quebec, Canada, August 2-6, 1965.

P. Cahill, L. P. Gold, and N. Owen, "The Microwave Spectrum of Methyl Vinyl Ether," Eighth European Congress on Molecular Spectroscopy, Copenhagen, Denmark, August 14-20, 1965.

P. Feldman, M. Levitt, S. Manson, R. Novick, and G. Sprott, "Zeeman Quenching of the $(1s2s2p)^4P_{5/2}$ Metastable State in Lithium," Zeeman Centennial Conference, Zeeman Laboratorium der Universiteit van Amsterdam, Amsterdam, Netherlands, September 6-11, 1965.

CRL Resonance Seminars

Meetings are held weekly at Columbia University, New York, N. Y. during the academic year, and are open to all members of the Physics Department. Guest speakers are invited to discuss work in the general area of the research in the Columbia Radiation Laboratory.

J. Dolan, Harvard University, "Polarization of Celestial X-Rays," July 9, 1965.

H. Kleinpoppen, University of Tübingen, Germany, "Low Energy Electron-Atom Collision Experiments," July 29, 1965.

ABSTRACT

Recent work has shown that under many experimental conditions, the decay of an ensemble of excited atoms is characterized by several relaxation times. Physically, these are the lifetime of the population of excited atoms, the lifetime of the average magnetic dipole moment (or orientation), the lifetime of the average electric quadrupole moment (or alignment), and the lifetimes of higher atomic multipole moments. Each multipole moment of the excited atoms decays with a characteristic lifetime because of the isotropy of the surrounding medium. In the limit of low vapor pressure, all of these lifetimes reduce to the natural radiative lifetime of the atom. In level-crossing experiments one can measure the lifetime of orientation and alignment separately. This is in contrast to classical nuclear magnetic resonance experiments, where only one parameter can be measured. The added flexibility in level-crossing experiments arises from the possibility of measuring the polarization of the fluorescent light. The existence of two lifetimes has been observed in Hanle-effect signals from the first $^3P_1{}^\circ$ state in lead when the signal was subject to resonant self-broadening, and also in the presence of foreign gas broadening and coherence narrowing.

Radiation due to the impact of very slow helium ions on the rare gases has been observed. The dependence of the cross section on the kinetic energy of the He^+ beam shows unexpected and important features down to the lowest energies studied (5 eV). The absolute cross sections are typically of the order of 10^{-16} cm^2 and in some cases are almost an order of magnitude larger. In at least one case, the radiation has been shown to result from charge exchange with simultaneous excitation.

Systematic observations have been made on the spectra of 6328Å light scattered from carbon dioxide near the critical temperature T_c and the critical density ρ_c. These studies were made as a function of both scattering angle θ and temperature T using an f/7 collecting lens. A new optical system has been developed which uses a lensless geometry and is capable of defining scattering angles to an accuracy better than ± 10' of arc without any averaging effects of a collecting lens.

I. ATOMIC PHYSICS

A. PROPERTIES OF THE METASTABLE STATE OF SINGLY IONIZED HELIUM

1. Direct Detection of the Two-Photon Decay Mode*
(M. Lipeles, R. Novick, N. Tolk)

We have collected all of the data relating to the two-photon decay experiment and have prepared for publication a paper on this subject. Figures 1, 2, and 3 present this data. Figure 1 shows a definite threshold at electron bombarding voltage of 65 V for both single events and coincidence counts. Figure 2 shows the expected dependence on microwave power with a background at full power for the single events only. These two observations along with the agreement of the experimental results with the calculated angular distribution, shown in Fig. 3, support the conclusion that we have observed the two-photon decay of singly ionized helium.

Construction of a large liquid-helium trap has been completed. However, installation of this trap has been postponed awaiting the arrival of new "soft" uv phototubes which will subtend larger solid angles. The excitation of the background gas by very low-energy helium ions has been expanded into a separate experimental endeavor. Future work on this project will be concentrated on measurements of the spectrum of the two-photon decay.

*This research was also supported by the National Aeronautics and Space Administration under Grant NsG-360.

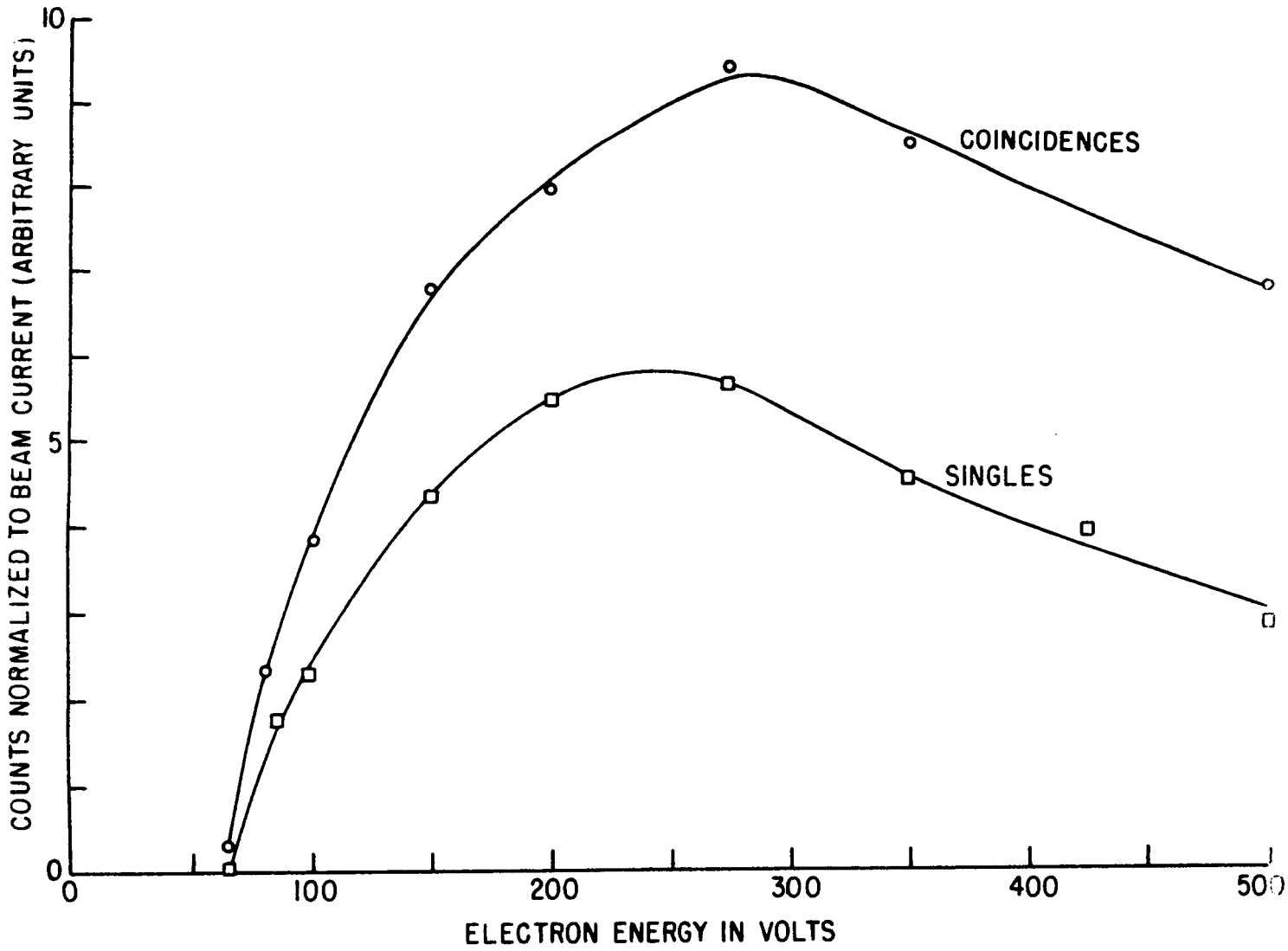

Fig. 1 Dependence of the coincidence counting rate and the rf induced singles counting rate on electron bombarding energy.

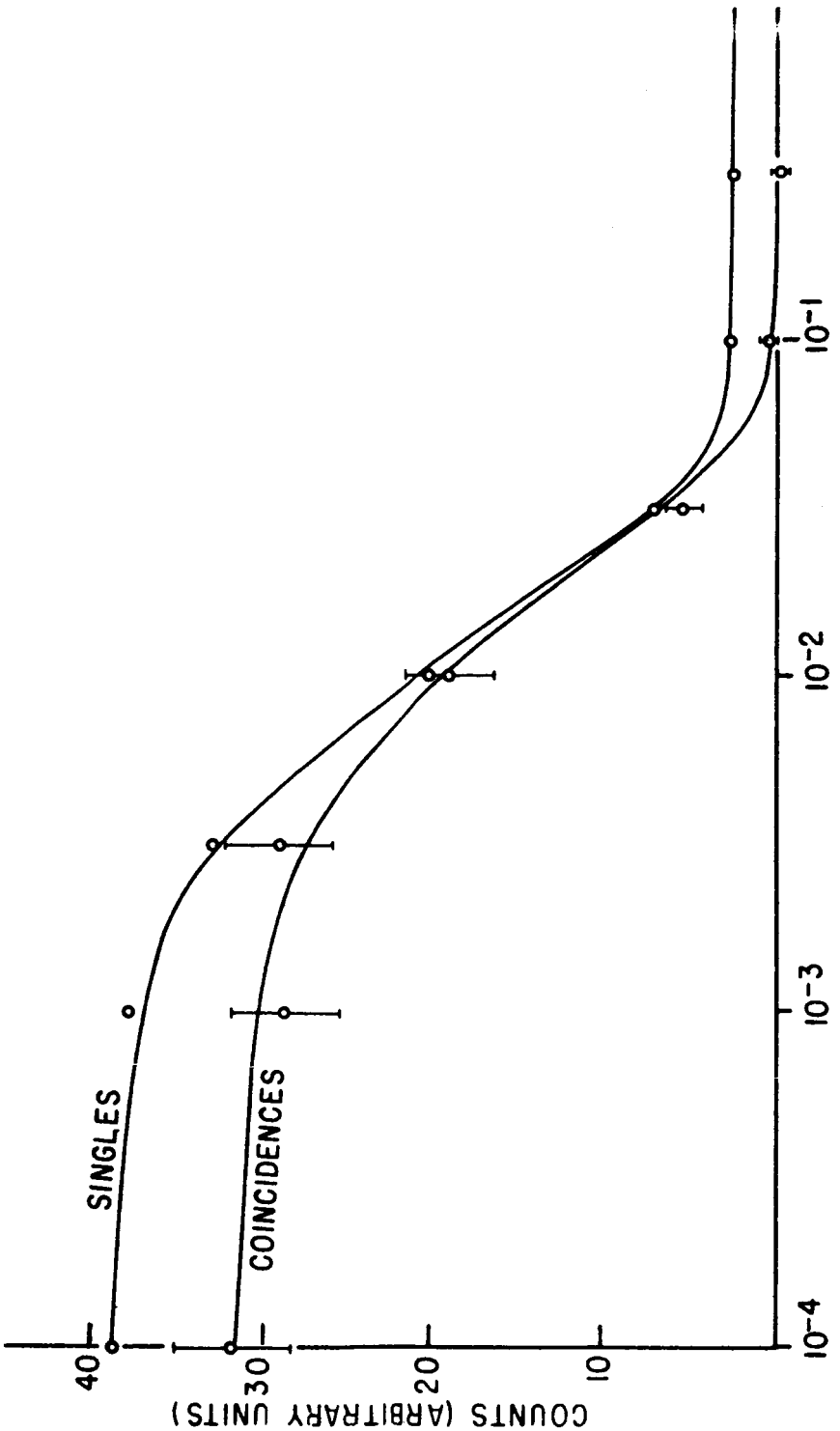

Fig. 2 Dependence of the coincidence and singles counting rate on rf quenching power.

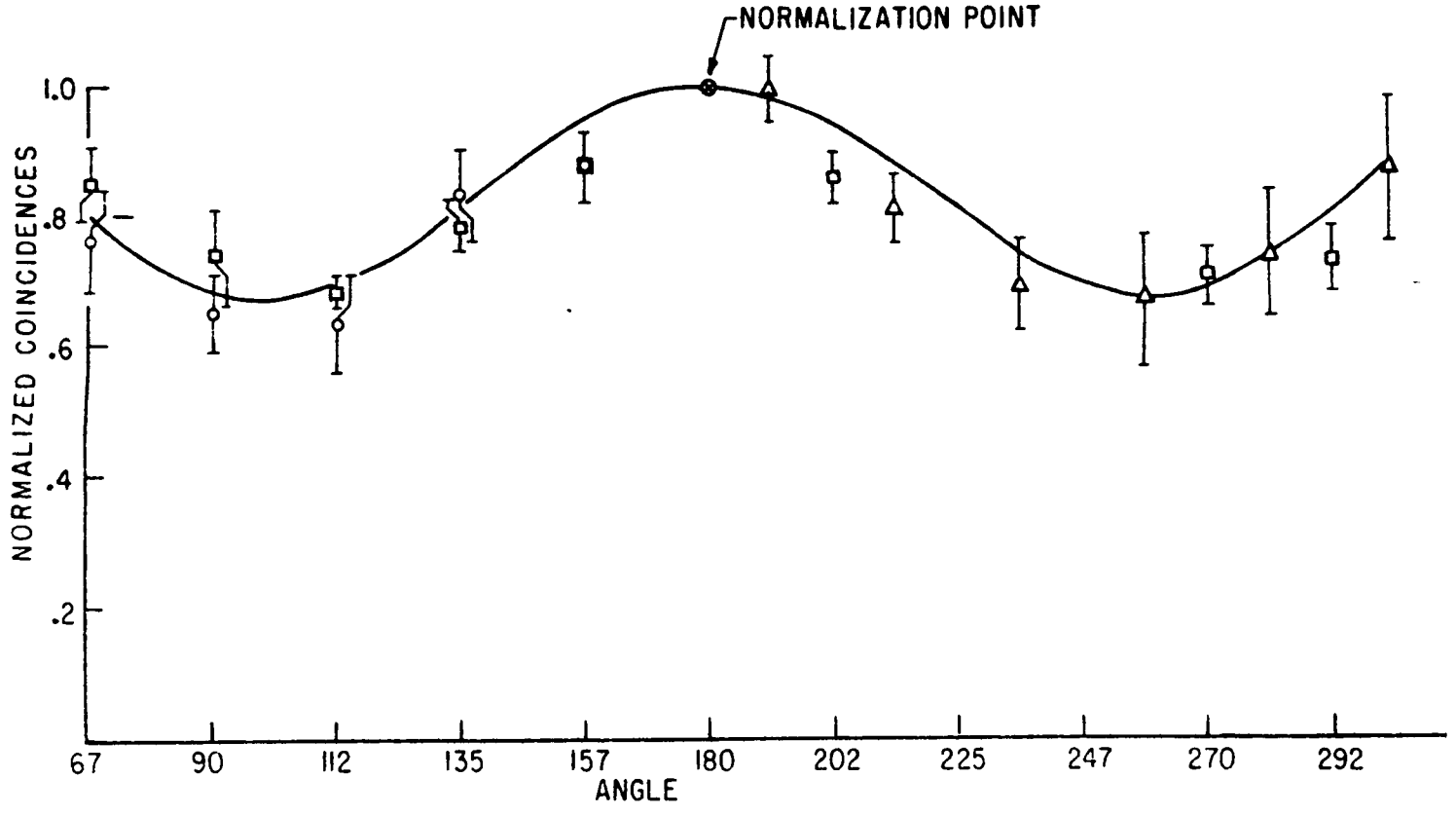

Fig. 3 Dependence of the coincidence counting rate on the angular separation of the photodetectors.

2. Direct Lifetime Measurements*
(S. Fisher, M. Lipeles, R. Novick, N. Tolk)

The drift tube vacuum chamber has been successfully evacuated and leak tested. During the next quarter the differentially pumped sliding seal will be assembled and tested.

*This research was also supported by the National Aeronautics and Space Administration under Grant NsG-360.

B. OPTICAL EXCITATION WITH LOW-ENERGY IONS*

(S. Dworetsky, M. Lipeles, R. Novick, N. Tolk)

As a result of studying the background radiation in the two-photon decay experiment (see Sec. A.1), it was observed that radiation arose from the impact of 10-eV He^+ ions on N_2 molecules. In order to study a more simple system the rare gases were chosen as targets. We have observed radiation due to the impact of very slow helium ions on Ar, Kr, Xe, and Ne. The dependence of the cross section on the kinetic energy of the He^+ beam shows unexpected and important features down to the lowest energies studied (5 eV). The absolute cross sections are typically of the order of 10^{-16} cm^2 and in some cases are almost an order of magnitude larger. In at least one case the radiation has been shown to result from charge exchange with simultaneous excitation. Previous studies of optical excitation by ion impact have been performed at much higher energies and have not revealed the structure at the lower energies. Simple arguments show that the radiation does not result from <u>direct</u> Coulomb excitation, but must involve pseudo level crossings in the ion-atom molecular collision complex. Aside from their intrinsic interest, these results have important bearing on plasma and atmospheric phenomena.

The apparatus used for the metastable He^+ experiment is being employed. The photons are detected with either a broad-band windowless EMI 9603 particle multiplier which responds from about 200Å to about 1200Å, a broad-band LiF window EMR 541-F "solar blind" photomultiplier which responds from 1050Å to 3500Å, or a 0.5-m Jarrell-Ash Ebert grating monochromator with quartz optics, together with a phototube with S-13 spectral response. The EMI and EMR tubes are mounted in the collision chamber, and their photocathodes are located about 5 cm from the ion beam. Absolute values for the cross sections obtained with these two tubes are estimated to within a factor of ten. The absolute as well as relative cross sections and their respective beam energy dependences show marked differences between the two ultraviolet regions. The cross sections for "soft" photon production vary from 3×10^{-20} cm^2 to 1×10^{-17} cm^2, while the "hard" photon cross sections are larger in the 10^{-18} cm^2 to about 10^{-15} cm^2 range.

Because the flux of photons incident on the monochromator is low, the entrance and exit slit openings must be relatively large in order to allow sufficient light through the instrument. Measurements are taken at a slit width of 2 mm resulting in a resolution of about 20Å. Through the use of this instrument for the case of the helium ion incident on argon, radiation in the visible region has been positively identified as arising from transitions in the Ar^+ spectrum. This suggests the radiative charge transfer reaction

$$He^+ + Ar \rightarrow He + Ar^{+*} \quad .$$

Spectral lines have been observed arising from many argon ion excited states: among them, the $^4p^4D^o$, $^4p^2D^o$, and $^4p^2P^o$ states. The possibility that the helium atom may also be formed in excited states has not been ruled out. Positive identification of the radiation from the collision of He^+ with Ne, Kr, and Xe is now in progress.

Program for the next interval: 1. To identify further states involved in these processes. 2. To construct a new apparatus specifically designed for this work. 3. To obtain a vacuum ultraviolet monochromator to extend the range of state identification to include regions now only covered by broad-band detectors.

*This research was also supported by the National Aeronautics and Space Administration under Grant NsG-360.

C. ELECTRIC-FIELD HANLE EFFECT

(W. Happer, A. Khadjavi, A. Lurio)

Level-crossing experiments on cadmium in parallel electric and magnetic fields have been completed, and the value for the differential polarizability in the first $^3P_1$ state was found to be

$$\frac{\alpha}{h} = 2515 \pm 75 \ \frac{\text{cps}}{(\text{kV/cm})^2} \ .$$

The basic experimental arrangement was identical to that used with mercury.[1] A gas-heated aluminum oven was used to maintain the resonance cell at 200°C, and an Osram lamp provided exciting light. The signal-to-noise ratio was typically 4 to 1 in contrast to signal-to-noise ratios of around 100 to 1 for

mercury. Instabilities in the Osram lamp were the chief source of noise. The level-crossing signals were better resolved than in the mercury experiments because of the longer lifetime of the $^3P_1$ state in cadmium. Electric field strengths up to 50 kV/cm were used, and the quadratic electric field dependence of the differential Stark shift was confirmed to within experimental error. At higher electric fields, the $\Delta m = 1$ level-crossing signals were much weaker than the corresponding signals at lower electric fields. Also the signal for one direction of the magnetic field was weaker than the signal for the opposite direction. We attribute these effects at high electric fields to a slight misalignment of the directions of the electric and magnetic fields.

Program for the next interval: We intend to work on level-crossing effects in the excited states of the alkali metals. Since the hyperfine splittings of these states are not much greater than the natural linewidth, some changes in our present experimental technique will be necessary.

(1) CRL Quarterly Progress Report, March 15, 1965, p. 5.

D. FINE STRUCTURE OF SINGLY IONIZED LITHIUM*

(T. Lucatorto, R. Novick)

During this quarter effort has been directed toward minimizing spurious signals generated by rf power. The newly developed rf loop has eliminated rf breakdown and has considerably reduced the interaction of the rf radiation with the electron beam. These favorable indications were observed with a lithium beam which lacked the intensity to permit any resonance measurements.

An attempt was made to use magnetic field modulation. The modulation was achieved by superimposing a small ac voltage onto the reference channel of the current regulator which supplies the dc current for the Zeeman magnetic field. The inductance of the Helmholtz coils unduly restricted the amplitude of the modulation. A separate set of modulation coils and power supply will be installed and tested.

Modulation of the magnetic field or rf power produces unwanted modulation in the total beam current. A differential amplifier which provides a high-gain negative feedback from the electron collector to a current-controlling grid was installed and was found to eliminate about 80% of the beam-current variation.

Program for the next interval: The efficacy of the new loop in producing resonance signals will be fully investigated.

*This research was also supported by the National Aeronautics and Space Administration under Grant NsG-360.

E. METASTABLE AUTOIONIZING ATOMS*

(L. M. Blau, P. Feldman, A. T-M. Kung, M. Levitt, R. Novick, G. Sprott)

1. Metastable Alkali Atoms

The experimental method used in the measurement of excitation functions and energy thresholds of the metastable autoionizing states in the alkali atoms was described in the previous Quarterly Progress Report.[1] The use of an oxide-coated cathode for the electron source and the calibration of the energy scale by means of comparison with the known excitation energies of the metastable states in He and N_2 allowed us to obtain an absolute

energy determination to within an uncertainty of ±0.3 eV. Here, we shall summarize the results of these measurements and, in addition, consider the problem of the identification of the observed structure of the excitation function in the case of lithium.

The excitation functions for lithium, potassium, rubidium, and cesium are shown in Figs. 4-7, respectively. In the case of sodium, the poor signal-to-noise ratio obscured the details of the structure, and only the principal threshold was determined. The cesium excitation function is actually a superposition of two different excitations, that of the metastable autoionizing state and that of the low-lying radiating state of Cs^+. This phenomenon was discussed previously,[2] and the results have been confirmed by additional data taken with a photosensitive detector.

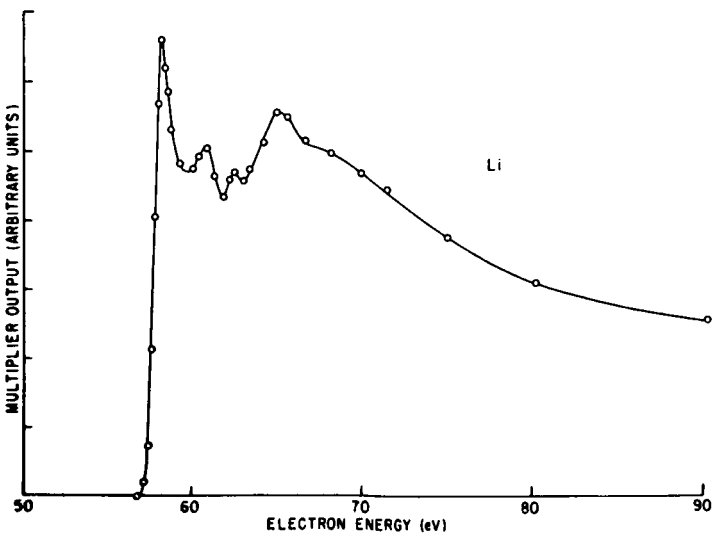

Fig. 4 Excitation functions of metastable autoionizing atomic states in lithium. The detector output is plotted as a function of the incident electron energy at constant bombarding current.

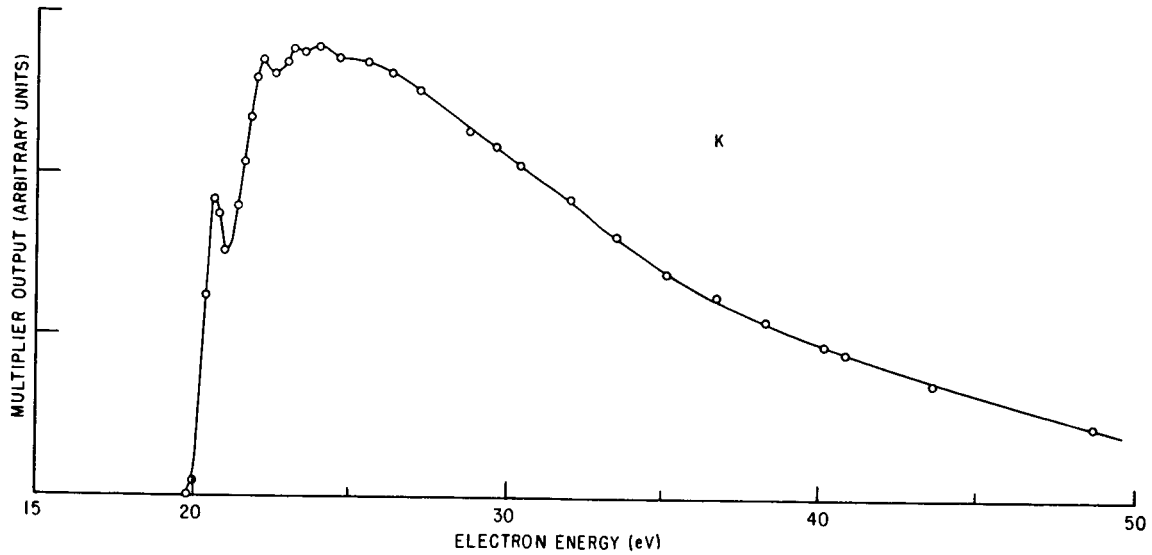

Fig. 5 Excitation function of metastable autoionizing atomic states in potassium.

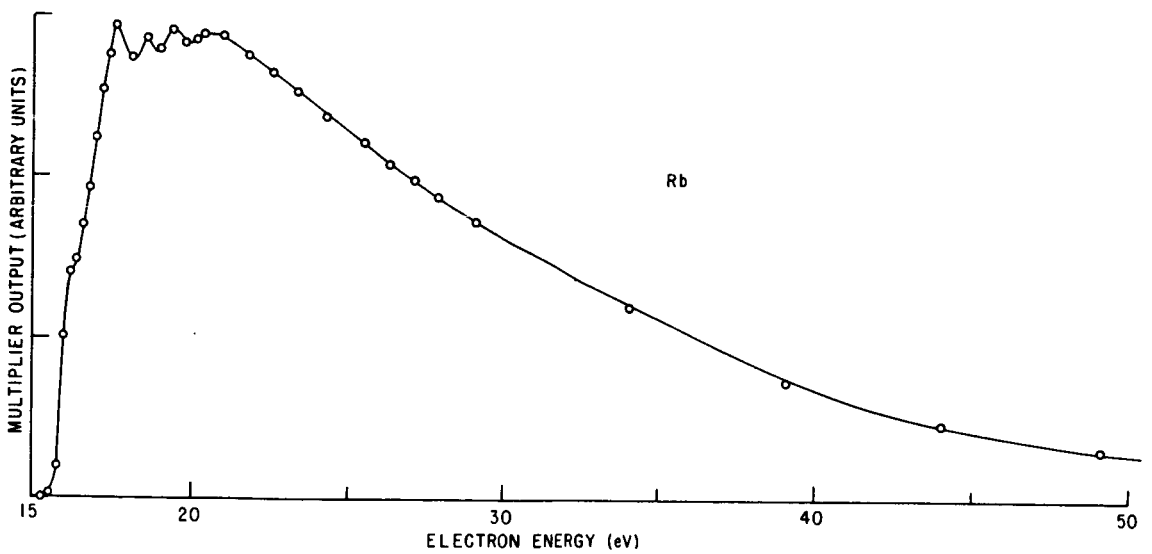

Fig. 6 Excitation function of metastable autoionizing atomic states in rubidium.

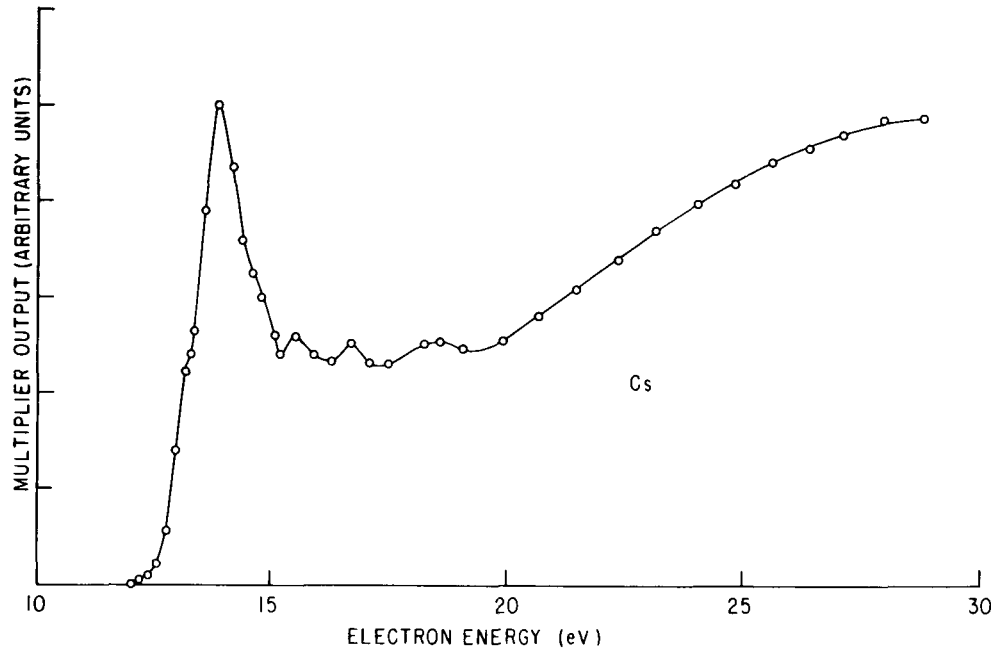

Fig. 7 Excitation function of metastable autoionizing atomic states in cesium.

A summary of the various excitation thresholds and the corresponding configurations is given in Table I. The right-hand column of the table gives the term and energy (in eV) of the lowest doublet state of the same configuration as determined from the ultraviolet absorption spectra of Beutler and Collaborators.[3] In the heavier alkalis the ordering of the possible metastable states is uncertain since the energy of an s electron with high principal quantum number is often depressed below that of an electron within a high angular momentum state with lower principal quantum number.

TABLE I

Measured Excitation Energies of the Lowest Metastable Autoionizing State in Each of the Alkali Atoms.

	Energy above Ground State	Assignment	Lowest Doublet State of Same Configuration Identified by Beutler and Collaborators[3]
Li	57.3 ± 0.3 eV	$(1s2s2p)\,^4P$	Not investigated
Na	31.8 ± 0.3 eV	$(2p^5 3s3p)\,^4D$	
K	19.9 ± 0.3 eV	$(3p^5 4s3d)\,^4F$	> 20 eV (beyond low-λ limit of apparatus)
Rb	15.8 ± 0.3 eV	$(4p^5 5s4d)\,^4F$	17.2 eV
Cs	12.6 ± 0.3 eV	$(5p^5 6s5d)\,^4F$	14.1 eV

In the case of lithium, calculations of the energy of some of the metastable autoionizing states are available, and the ordering of the lowest quartet states is known. Table II lists the calculated energy values according to several authors.[4-8] The recent variational results of Minn,[5] Manson,[6] and Holøien,[7] if considered as upper bounds to the true energy eigenvalue of the $(1s2s2p)\,^4P$ state, give excellent agreement with the experimental value of 57.3 ± 0.3 eV. As for the details of the structure on the Li excitation curve, in Table III the four distinct thresholds, consecutively numbered, are listed and tentatively identified. This is done on the assumption that

TABLE II

Calculated Energies of the Lowest Metastable Autoionizing States in Lithium (in eV above the ground state).

Li Level	A	B	C	D	E
$(1s2s2p)^4P$	57.99	57.63	57.52	57.6	55.47
$(1s2p2p)^4P$	61.42				59.67
$(1s2s3s)^4S$					61.11
$(1s2s3p)^4P$					61.75
$(1s2s3d)^4D$					61.80
$(1s2p3s)^4P$					63.17

A. Ta-You Wu and S. T. Shen, ref. 4 (3 parameter hydrogenic orbitals wave function)

B. S. Manson, ref. 6 (15 parameter Hartree-Fock type wave function)

C. F. Minn, ref. 5 (15 parameter configuration interaction wave function)

D. E. Holøien, ref. 7 (Hylleraas type variational wave functions)

E. J. D. Garcia and J. E. Mack, ref. 8 (Screening parameter evaluation)

TABLE III

Energy Thresholds of Metastable Autoionizing States in Lithium

Threshold	Energy	Tentative Assignment
1	57.3 eV	$(1s2s2p)^4P$
2	59.9 eV	$(1s2p^2)^4P$
3	61.9 eV	$(1s2s3s)^4S$
4	63.2 eV	$(1s2s3p)^4P$, $(1s2s3d)^4D$, $(1s2p3s)^4P$, $(1s2p3p)^4P$, ^4D

higher-lying quartet states may radiate to the lowest quartet states in times shorter than the autoionization lifetimes, so that the higher metastable autoionizing states are observed through their radiative cascade to the $(1s2s2p)^4P$ state. Such transitions have been hypothesized as the source of several unassigned lines in the emission spectrum of Li^+ as reported by Herzberg and Moore.[9] The energies and tentative assignments listed in Table III are used to deduce primary allowed transitions which are listed in Table IV. The fourth column gives the possible corresponding line in units of both wavelength and energy from the optical data, and it can be seen that a correspondence between the two is possible. On the other hand, for a positive identification, it would be necessary to observe the radiation and the production of metastable atoms simultaneously to establish that the initial state in the transition actually lies below the first excited state of Li^+. Garcia and Mack[8] have made an identification of these lines on the basis of their calculated energies. Their assignments differ from ours, and the discrepancy may be traced to the fact that their energy for the $(1s2s2p)^4P$ state lies 1.8 eV below our present measurement.

TABLE IV

Possible Radiative Transitions Between Metastable Autoionizing States in Lithium

Transition	ΔE	Tentative Assignment	Herzberg-Moore[9]
2 - 1	2.6 eV	$(1s2s2p)^4P$ - $(1s2p^2)^4P$	4607Å (2.69 eV)
3 - 1	4.6 eV	$(1s2s2p)^4P$ - $(1s2s3s)^4S$	2934Å (4.22 eV)
4 - 1	5.9 eV	$(1s2s2p)^4P$ - $(1s2s3d)^4D$	2336Å (5.31 eV)
		$(1s2s2p)^4P$ - $(1s2p3p)^4D$	
4 - 2	3.3 eV	$(1s2p^2)^4P$ - $(1s2p3s)^4P$	3714Å (3.34 eV)

No further work on this aspect of our investigation of metastable autoionizing states is planned. An article reporting the results of this work is being prepared for publication.

2. Rf Spectroscopy

A set of experiments has been initiated this quarter on the basis of the experimental possibilities which were indicated by a new calculation of the metastable level scheme.[6] The results of this calculation have permitted us to understand the results of an experiment[10] on the Zeeman quenching of the $(1s2s2p)^4P_{5/2}$ state of Li^7. It was found that the structure observed on the quenching curve corresponded to the anticrossing of long-lived J = 5/2 states with either J = 1/2 or J = 3/2 states, which are coupled more strongly to the continuum. The two states interact through off-diagonal ($\Delta J = 1$) hyperfine and Zeeman matrix elements.

The success of the theory in predicting the correct anticrossing H fields indicates that it can also be utilized to predict splittings for rf resonance work. An experiment which is then immediately suggested is the determination of the high-field splittings of the pairs of anticrossing states. Such states are known to have appreciably different lifetimes and energy separations near the anticrossing point which are small enough to permit use of high-power low-frequency rf generators. The new eigenfunctions can be used to calculate the rf coupling between the two states at H fields just below (or above) the anticrossing point. These eigenfunctions also indicate that the detection of microwave induced transitions between the F = 4 and F = 3 hyperfine levels, on which we have been working,[11]

is difficult even at high magnetic fields because of the small differential metastability of the states. The observation of the aforementioned fine-structure resonances, however, will permit us to make the adjustment of the theory necessary to predict accurately the hyperfine splittings, thus rendering the latter experiment more feasible.

The proposed experimental setup will utilize almost all of the existing components of the old resonance apparatus with a major modification in the beam detection system. The Bendix multiplier, which is restricted in operation to magnetic fields of the order of 400 G, will be replaced by a field-independent surface-barrier solid-state detector. Electrons from the decay of the metastable lithium beam will drift out of the beam region due to an electric field of about 100 V, which is designed to minimize the background signal. It is thought that the observed background is caused by the electric-field-induced ionization of discrete states lying just below the ionization limit.[12] The electrons will then be accelerated in a high-field ($\approx$15 keV) region so that they have sufficient energy to be clearly identified by the pulses they give rise to in the solid-state detection system. This system will consist of the cooled surface-barrier detector, a very low-noise charge-sensitive preamplifier, and a matching amplifier. For resonance work, this system will be used in conjunction with a dual-mode scalar. Mode one will operate in the presence of an rf field, while mode two will operate when the rf field is absent. The difference in the number of counts in the two modes will indicate whether or not a transition between the long-lived and short-lived states has occurred for a particular frequency of the rf field.

As an initial check on this apparatus, and to test more sensitively our theory, we will repeat the Zeeman quenching experiment. Since the experimental configuration involves one uniform H field for metastable production, quenching, and detection, the positions and widths of the anticrossings can be obtained with greater accuracy than in the original experiment. We will also have the additional degree of freedom afforded by a movable detector. It is also hoped to determine roughly the lifetimes of the various levels, and to note any bombardment polarization effects (unequal populating of the several M_F levels), by fitting a theory incorporating the eigenfunctions and assumed lifetimes to quenching data obtained for several metastable excitation energies.

The components of the apparatus described above are presently being constructed and assembled, and we will proceed with the experiments which we have outlined during the next quarter.

3. He^- Ion

Studies of the He^- ion analogous to the investigations of the metastable states in the alkali elements are being initiated as part of the Laboratory's continuing interest in metastable autoionizing atoms and ions in general. In addition, there is a good possibility that the mechanism of differential metastability may be utilized to produce a source of polarized $^3He^-$ ions.[13] The development of such an ion source for tandem Van de Graaff generators would be a valuable tool for nuclear structure studies.

The first step in the present research program is to study the $^4He^-$ ion and to measure the effect of magnetic fields on the mixing of the various magnetic substates of the $^4P_{5/2}$ component of the ion. Since the atomic properties of ^4He and ^3He are very similar, the more abundant $^4He^-$ ion will be studied first in order to determine the feasibility of producing a polarized $^3He^-$ ion beam.

According to the selection rules only the $^4P_{5/2}$ state is metastable, having a lifetime in the millisecond region,[14] while the $^4P_{3/2}$, $^4P_{1/2}$, $^2P_{3/2}$, and $^2P_{1/2}$ states are much shorter lived.[15] Hence, any mixing of the metastable $(J, M_J) = (5/2, M_J)$ states with the shorter-lived $(3/2, M_J)$ and $(1/2, M_J)$ states caused by an external magnetic field will result in a decrease in beam intensity. Similar experiments have been completed on the $(1s2s2p)^4P$ metastable state in Li^7, and the positions of anamolies in the Li quenching curve[10] (plot of beam intensity vs external magnetic field) have been identified as anticrossings of the substates of the $(1s2s2p)^4P$ state (see Section 2). By comparing the measured quenching curve of $^4He^-$ with that of Li, it is felt that limits on the lifetimes of the $^4P_{3/2}$ and $^4P_{1/2}$ states can be obtained.

The $^4He^-$ beam may be produced by a Cockcroft-Walton accelerator, and measurements of beam intensity and dispersion are now being initiated. This machine should produce a sufficiently intense beam of $^4He^-$ ions in the energy range of 10 keV $\leq E \leq$ 100 keV. Combining this relatively high beam energy with a metastable lifetime in the millisecond region necessitates the use of long flight paths (of between 5-10 m) in order to obtain measurements with a few percent uncertainty. In addition to

this problem of long flight paths, a magnetic field of about 20,000 G will be necessary in order to achieve the desired degree of mixing of the magnetic substates. These two problems have been solved by utilizing the old cyclotron magnet of the obsolete 19-MeV proton cyclotron of Columbia University. With slight modifications the magnet may be made to produce a magnetic field of 20,000 G over an area 30 inches in diameter. By trapping the $^4He^-$ ions in this field and causing them to follow vertical helical paths, the over-all flight path may be made to approach 10 m.

Once reasonable estimates of the $^4P_{3/2}$ and $^4P_{1/2}$ lifetimes are established, the feasibility of producing a polarized $^3He^-$ ion source can be fruitfully examined.

*This research was also supported by the National Aeronautics and Space Administration under Grant NsG-360.

(1) CRL Quarterly Progress Report, June 15, 1965. p. 7.

(2) CRL Quarterly Progress Report, September 15, 1964, p. 9.

(3) H. Beutler, Z. Physik 86, 495 (1933); 91, 131 (1934); H. Beutler and K. Guggenheimer, Z. Physik 87, 176 (1933); 88, 25 (1934).

(4) Ta-You Wu and S. T. Shen, Chinese J. Phys. 5, 150 (1944).

(5) F. Minn, to be published.

(6) S. Manson, private communication.

(7) E. Holøien, private communication.

(8) J. D. Garcia and J. E. Mack, Phys. Rev. 138, A987 (1965).

(9) G. Herzberg and H. R. Moore, Can. J. Phys. 37, 1293 (1959).

(10) P. Feldman, Ph.D. Thesis, Columbia University, 1964 (unpublished).

(11) CRL Quarterly Progress Report, June 15, 1965, p. 11.

(12) A. C. Riviere and D. R. Sweetman, Proc. Fifth International Conference on Ionization Phenomena in Gases, Munich 1961, North-Holland Publishing Co., p. 1236.

(13) P. Feldman and R. Novick, "Polarization of He^3 Negative Ions," Compt. Rend. Congr. Intern. Phys. Nucl., Paris, 2, C144, p. 785 (1964).
(14) J. L. Pietenpol, Phys. Rev. Letters 7, 64 (1961).
(15) E. Holøien and J. Midtdal, Proc. Phys. Soc. (London) A68, 815 (1955).

F. HYPERFINE STRUCTURE OF GROUP IIA ISOTOPES*

(R. Novick, M. Swagel)

During this quarter five natural barium cells have been tested. All cells had latticed window flanges. The first three cells, with bodies of 304 stainless steel, 305 stainless steel, and molybdenum, respectively, were operated at temperatures up to 750°C. In these cells the Hanle effect in the $6^1P_1 - 6^1S_0$ (green) transition was strongest at 550°C, and the Hanle effect in the $6^3P_1 - 6^1S_0$ (red) transition started to appear at 750°C. After three hours of operation at 750°C, the windows became totally opaque.

The temperature of the next cell was limited to a maximum of 700°C. Again the Hanle effect was strongest at 550°C. The windows became opaque after six hours. The temperature of the fifth cell was limited to a maximum of 650°C. After fifteen hours of running, the temperature for maximum green Hanle effect dropped from 550°C to 450°C. The red Hanle effect appeared at 570°C with signal-to-noise ratio equal to 100. Double resonance in Ba^{138} was induced at 30 Mc with 2.5 A of rf current and S/N equal to 10. When the rf current was increased, an rf discharge was precipitated in the cell.

Program for the next interval: In previously constructed cells the barium plug was loaded in a bell jar and transferred in air to the bake-out vacuum system. An oxide layer formed on

the barium. This layer may be responsible for the difficulty in achieving Hanle-effect and double-resonance signals at the expected temperatures. For the next cell, the barium plug will be loaded with barium in the vacuum system used for evacuating the cell. Thus, the barium plug will not be exposed to air and no oxide layer will form.

*This research was also supported by the National Aeronautics and Space Administration under Grant NsG-360.

G. FINE AND HYPERFINE STRUCTURE OF THE 3P STATE OF Li^7*

(R. C. Isler, S. Marcus, R. Novick)

Measurements which are accurate to a few parts in 10^6 have been obtained for the magnetic fields at which the four $\Delta m = 2$ level crossings occur in the 3P state of Li^7. In terms of the resonance frequency of the proton probe used to measure these fields, they are

$$3911.446^{+0.013}_{-0.024} \text{ kc} ,$$

$$3901.757^{+0.005}_{-0.002} \text{ kc} ,$$

$$3892.166^{+0.006}_{-0.014} \text{ kc} ,$$

and

$$3882.649^{+0.005}_{-0.002} \text{ kc} .$$

Each value is the average of four measurements, and the uncertainties quoted are the largest observed deviations from the average.

The intervals between successive hyperfine crossings, again in terms of the proton resonance frequency, are

$$9.689^{+0.018}_{-0.026} \text{ kc} ,$$

$$9.591^{+0.011}_{-0.016} \text{ kc} ,$$

and

$$9.517^{+0.011}_{-0.016} \text{ kc} .$$

The variations in these intervals reflect the effects of second-order magnetic dipole and electric quadrupole interactions. Once a sufficient number of measurements have been made to reduce the statistical uncertainty in the measurements of the hyperfine splitting, it should be possible to extract a value for the electric quadrupole moment in Li^7.

Program for the next interval: Further measurements of the crossing fields will be made for the 3P state of Li^7, and similar experiments will be performed for Li^6.

*This work was also supported by the National Aeronautics and Space Administration under Grant NsG-360.

II. PROPERTIES OF RADIOACTIVE ATOMS

A. OPTICAL STUDIES OF ATOMS

(W. Happer, R. Novick, E. B. Saloman)

During this quarter, we have successfully carried out the experiments discussed in the last Quarterly Progress Report.[1,2] Different lifetimes for atomic states excited with linearly and circularly polarized light were observed when the Hanle-effect signal was subject to resonant self-broadening, and also in the presence of foreign gas broadening and coherence narrowing.

The general behavior of the linewidth[3] is indicated in Fig. 8, where the ratio of the quadrupole or alignment width ($\gamma_{al} = 1/\tau_{al}$) to the natural width $\Gamma = 1/\tau$ [$\tau = 5.75(20) \times 10^{-9}$ sec][7] has been plotted as a function of atomic vapor density. The results of measurements of the dipole or orientation width (γ_{or}) and the alignment width (γ_{al}) are summarized in Table V. Because of the fairly large f value for the 2833Å resonance line in lead, the linewidth at high vapor densities should be determined chiefly by resonant collision broadening.[4,5] The results

TABLE V. Results.

Lead Atomic Density (cm^{-3})	γ_{or}/Γ	γ_{al}/Γ	$(\gamma_{or} - \Gamma)/(\gamma_{al} - \Gamma)$ Experimental	$(\gamma_{or} - \Gamma)/(\gamma_{al} - \Gamma)$ Theoretical	Comment
2.9×10^{15}	1.99(3)	1.76(3)	1.30(5)	1.30 ↔ 1.67	a
1.3×10^{13}	1.36(2)	1.22(2)	1.64(18)	-	b
1.3×10^{13}	0.852(18)	0.818(18)	0.8(2)	0.714	c

a. These results are for the case of resonant self-broadening.
b. These results are for the case of foreign gas broadening.
c. These results are for the case of a saturated coherence-narrowing effect.

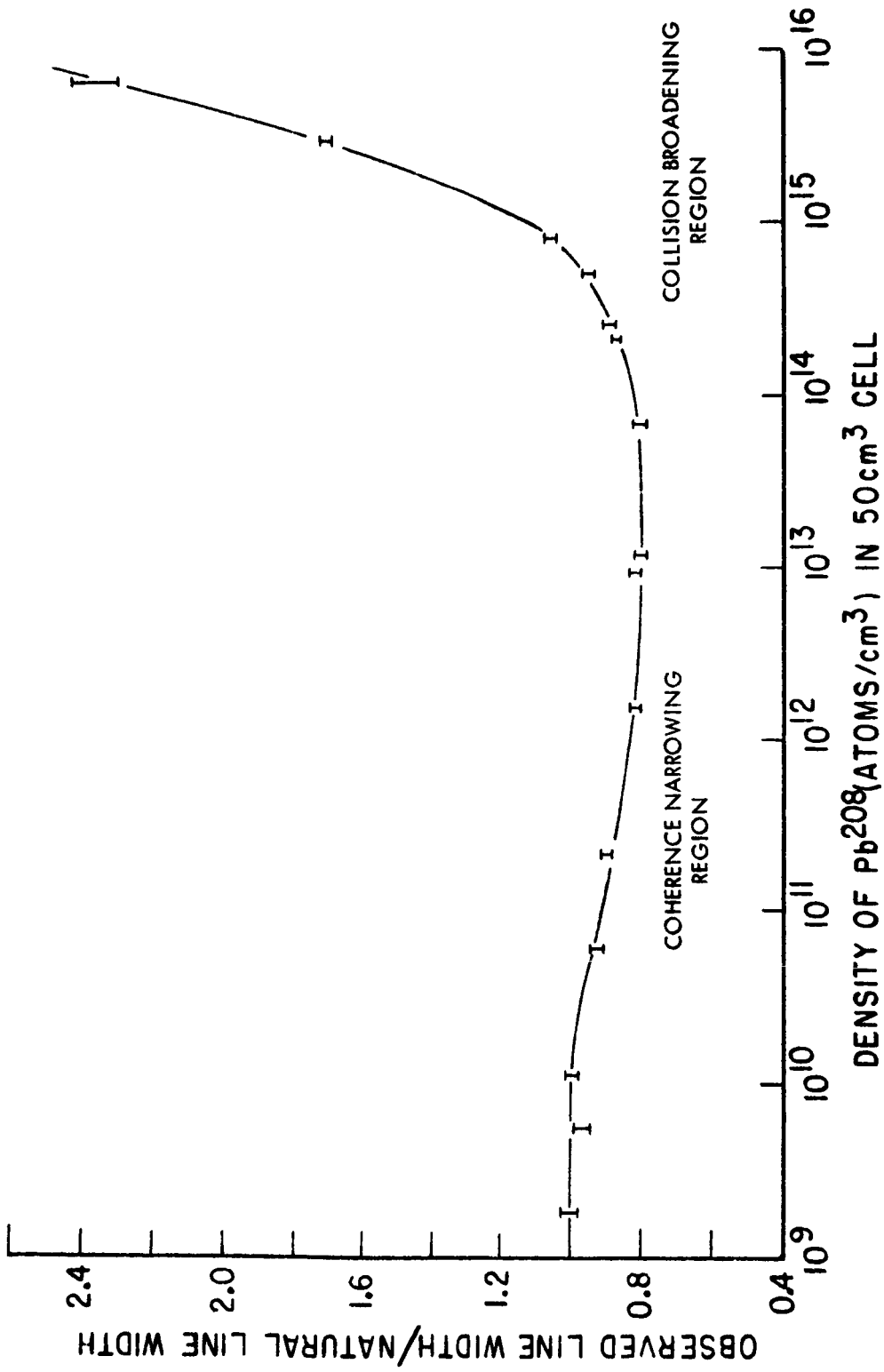

Fig. 8 Linewidth of $\Delta m=2$ Hanle-effect resonances in the $(6s^2 6p7s)\,^3P_1^o$ state of Pb^{208} $(1/\tau_{a1})$.

of our measurements are consistent with the rough theoretical estimates of Omont[5] for the ratio of the two relaxation times. A marked difference in γ_{al} and γ_{or} was also observed with a gassy resonance cell. The exact constituents and pressure of the foreign gas are unknown, but a spectrographic analysis of the light from a microwave discharge through the cell showed Ne, OH, CO, and NH emission bands as well as strong lines from atomic hydrogen. In the future we plan to carry out more controlled studies of foreign gas broadening.

Coherence narrowing in lead is much less pronounced than in atoms such as mercury because of the presence of branch decay modes from the excited state. One can show that the theoretical maximum branching ratio is reduced by the branching ratio [27(3)%][3] to the ground state. Since the coherence narrowing is so small, our experimentally measured values of γ_{al} and γ_{or} are nearly the same, but within experimental error our ratio of $(\gamma_{or} - \Gamma)/(\gamma_{al} - \Gamma)$ is in agreement with the theoretical ratio of 5/7.[6]

These experiments demonstrate that under a wide range of experimental conditions the different multipole components of the density matrix describing excited atoms in a vapor relax with measurably different time constants. More detailed studies of this kind should yield considerable information about the mechanisms involved in depolarizing collisions.

The above experiments indicated that the quartz cells used in these experiments often become gassy when heated above 750°C. As a result it was decided to repeat the resonant collision broadening measurements. In this series of measurements, the cells were kept at high temperatures for as short a period as

possible. The presence of foreign gas was monitored before and after a run by observing the linewidth at which the coherence narrowing saturated. The results are listed in Table VI, where the uncertainty is three times the standard deviation of the data.

TABLE VI

Results: Resonant Self-Broadening

T (°C)	N (cm^{-3})	Broadening (10^8 cps)	$\bar{v}\sigma$ (10^{-8} cm^3/sec)
750	2.00×10^{14}	0.058(22)	2.9(11)
800	5.10×10^{14}	0.159(27)	3.12(54)
850	1.17×10^{15}	0.388(27)	3.31(26)
903	2.65×10^{15}	0.858(40)	3.24(16)

Allowing for the uncertainty of the density determination from vapor-pressure curves, we obtain for the resonant collision broadening effect in the $(6p7s)^3P_1^o$ state of lead

$$\bar{v}\sigma = 3.3(4) \times 10^{-8} \text{ cm}^3/\text{sec} ,$$

where $\bar{v}$ is the mean relative velocity of the lead atoms, and σ is the resonant collision broadening cross section. This result is within the range of the predictions of Omont.[5]

A careful determination was made of the lifetime of the $(6s^26p8s)^3P_1^o$ state in lead. The energy levels of interest are shown in Fig. 9. Lead atoms were excited from the $(6s^26p^2)^3P_0$ ground state to this state by 2053Å resonance light. Hanle-effect resonances were observed in the 5201Å cross fluorescence to the $(6s^26p^2)^1S_0$ state. Eight determinations were made over

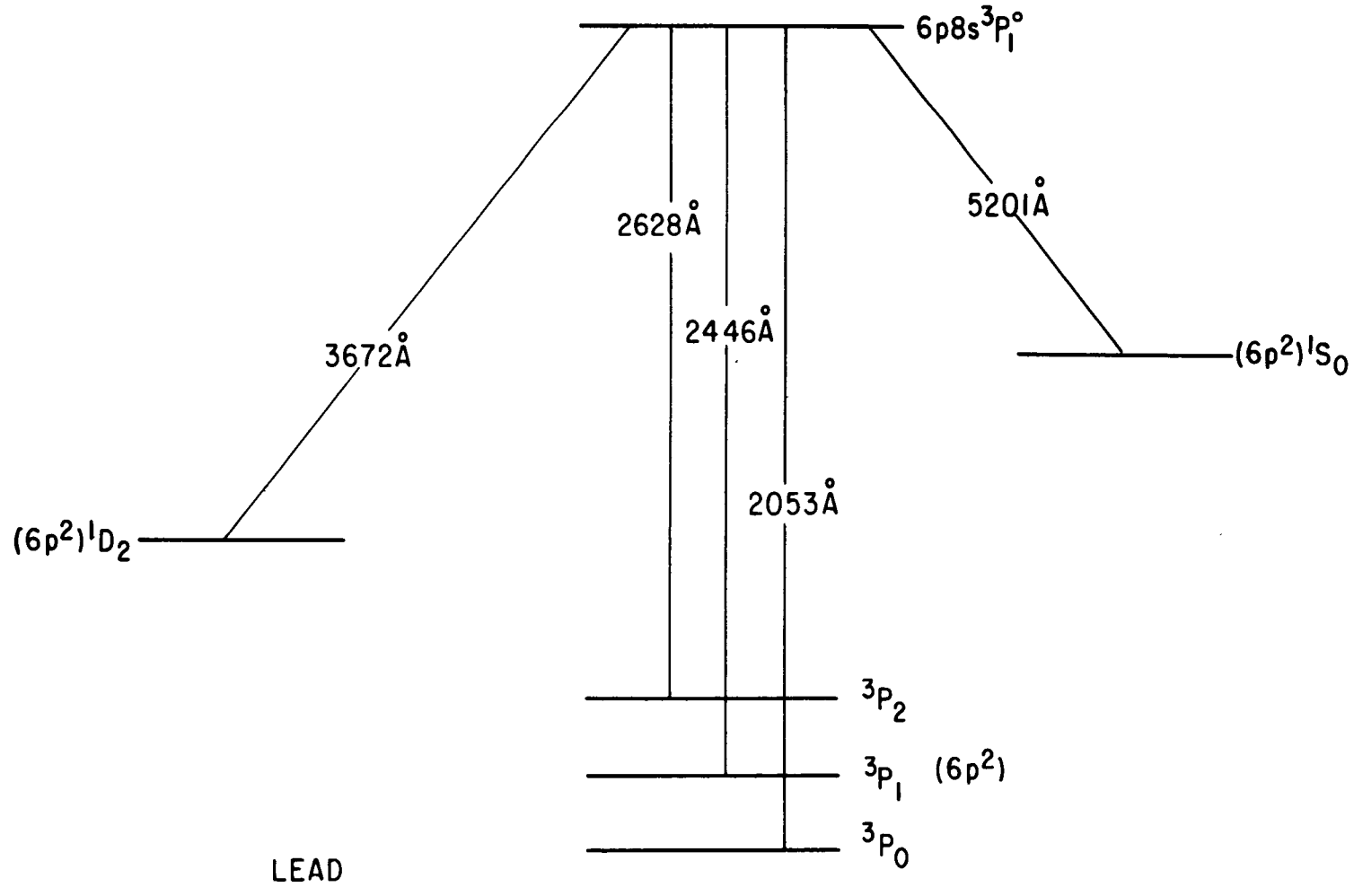

Fig. 9 Atomic energy levels of interest in the determination of the lifetime of the $(6p8s)^3P_1^\circ$ state in lead.

an atomic density range of 200. No significant coherence narrowing was observed. The weighted mean of these determinations gives, for the lifetime of the $(6s^2 6p8s)\,^3P_1^o$ state, the value

$$\tau = 1.29(14) \times 10^{-8} \text{ sec},$$

where the quoted uncertainty is three standard deviations.

A preliminary determination was made of the lifetime of the $(6s^2 6p7s)\,^1P_1^o$ state in lead. The energy levels of interest are shown in Fig. 10. Lead atoms were excited from the $(6s^2 6p^2)\,^3P_0$ ground state to this state by 2022Å resonance light. Hanle-effect resonances were observed in the 5005Å cross fluorescence to the $(6s^2 6p^2)\,^1S_0$ state. On the basis of the preliminary determination, we assign a value of

$$\tau = 4.7(6) \times 10^{-9} \text{ sec}$$

for the lifetime of the $(6s^2 6p7s)\,^1P_1^o$ state in lead. This value combined with our previous determination of the lifetime of the $(6s^2 6p7s)\,^3P_1^o$ state allows us to determine the Russell-Saunders coefficients for the mixing of these two states if we assume that the decay of the $^1P_1^o$ state is solely due to this mixing.[8] The preliminary values obtained are listed in Table VII together

TABLE VII

Preliminary Results

Russell-Saunders Coupling Coefficient	α	β
Preliminary value from lifetimes	0.563	0.826
Value calculated from deviation of energy levels from values predicted by the interval rule	0.533	0.847

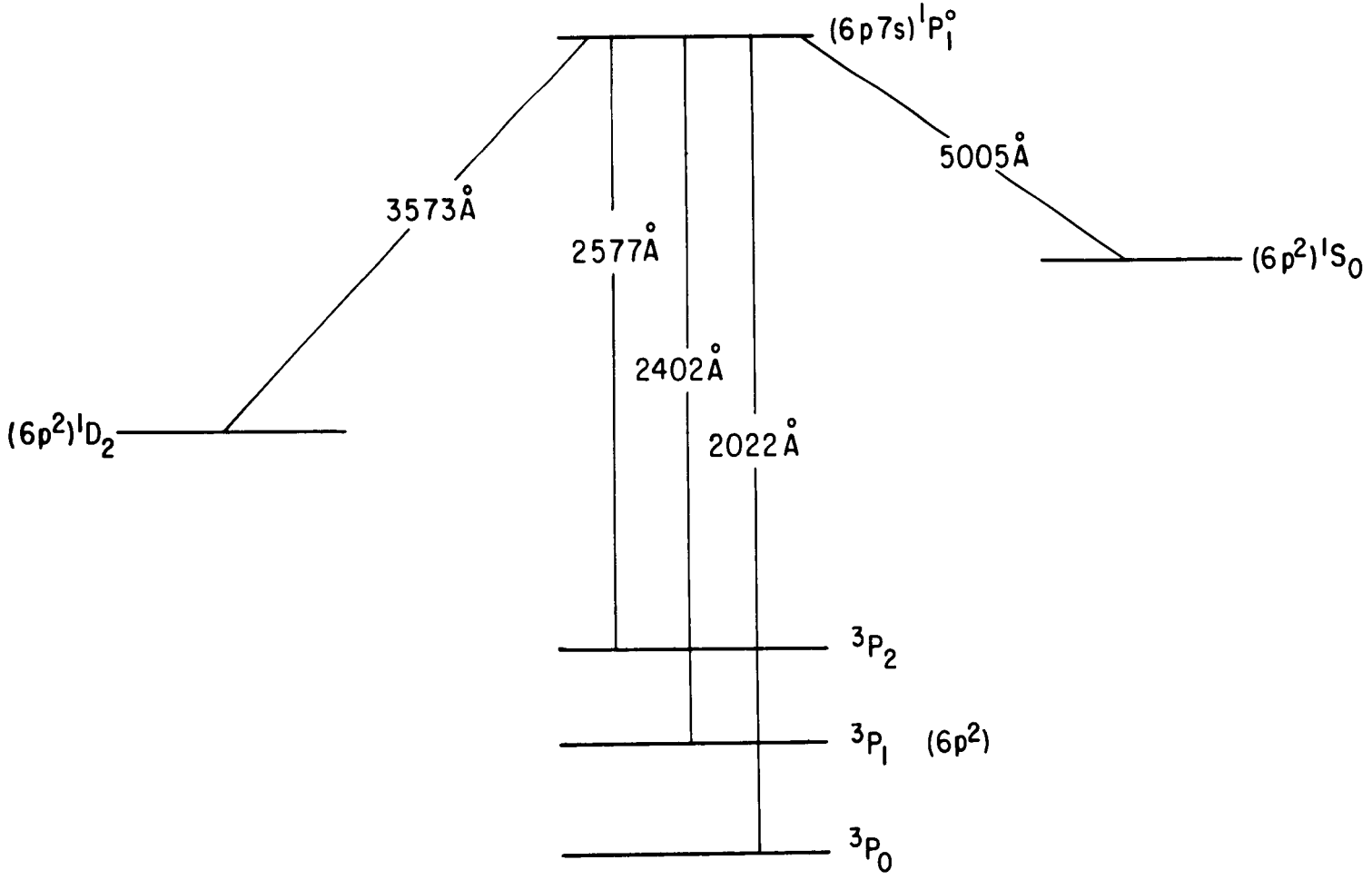

Fig. 10 Atomic energy levels of interest in the determination of the lifetime of the (6p7s)$^1P_1^o$ state in lead.

with the values obtained from the deviation of the energy levels from the positions predicted by the interval rule.

A study has begun of the possibility of using modulated light in detecting level-crossing resonances in place of the modulated magnetic field used at present. Modulated light has the advantages of showing the actual line shape rather than its derivative and of not requiring a series of different modulations to account for the effect of modulation broadening. It has the disadvantage of providing only a single peaked Lorentzian rather than a double peaked dispersion curve from which to determine the width of the level-crossing effect and of being almost a factor of two broader than the derivative curve.

It is very easy to modulate the flow lamp light source by modulating its rf exciter. The best signal-to-noise ratio was obtained when the lamp's rf was 100% modulated. Also, 280-cycle modulation produces better signal-to-noise ratio than either 37 cps or 13 cps modulation. Studies of the feasibility of this method of detecting level crossings are continuing.

(1) CRL Quarterly Progress Report, June 15, 1965, p. 20.
(2) W. Happer and E. B. Saloman, Phys. Rev. Letters 15, 441, (1965).
(3) E. B. Saloman and W. Happer, Bull. Am. Phys. Soc. 10, 596 (1965).
(4) F. W. Byron, Jr., M. N. McDermott, and R. Novick, Phys. Rev. 134, A615 (1964).
(5) A. Omont, J. Phys. Radium 26, 26 (1965).
(6) M. T. Dyakonov and U. T. Perel, Soviet Physics - JETP, 20, 997 (1965).
(7) R. Novick, B. W. Perry, and E. B. Saloman, Bull. Am. Phys. Soc. 9, 625 (1964); E. B. Saloman, Bull. Am. Phys. Soc. 10, 49 (1965).
(8) A. Lurio, M. Mandel, and R. Novick, Phys. Rev. 126, 1758 (1962).

III. PHYSICS OF MOLECULES

A. BEAM MASER SPECTROSCOPY*

(P. Cahill, L. P. Gold)

A mechanical beam modulator has been installed in the beam maser spectrometer between the crinkled-foil source and the electrostatic focusing field. By use of phase detection, the detection sensitivity of the spectrometer should be increased, and during the next quarter the hyperfine spectrum of the 3_{03}-3_{13} rotational transition in NH_2D at 43042 Mc will be re-examined.

*This research was also supported in part by the Air Force Office of Scientific Research under Grant AF-AFOSR-330-63, and in part by the Office of Naval Research under Contract Nonr-266(45).

B. MICROWAVE SPECTROSCOPY*

(P. Cahill, L. P. Gold)

Part I

A rotational transition has been observed in CsOH in a molecular beam electric resonance experiment at Harvard University[1] and subsequently at Columbia. Further attempts to observe this spectrum in our absorption spectrometer were unsuccessful. The original high-temperature microwave cell is being re-assembled, and another search for the microwave spectrum of CsOH will be made.

Part II

During this quarter the ground state and one of the first excited vibrational states of CD_3OCHCH_2 have been assigned. The

observed rotational constants agree very well with the ones calculated from the structure used to give the best fit for the normal cis species.

For the normal cis species of CH_3OCHCH_2, no splittings were observed in the assigned spectral lines, thus giving a lower limit to the barrier to internal rotation of the methyl group of about 2000 cal/mole. Three sets of vibrationally excited states of the normal species have been identified and assigned rotational constants. Table VIII summarizes the data obtained on all the excited states. The three low-frequency vibrations

TABLE VIII

Rotational Constants (Mc/sec) for Ground and Excited Vibrational States of cis Methyl Vinyl Ether.

CH_3OCHCH_2

	A	B	C	κ
v = 0	18225.06	6388.87	4875.95	-0.7733
v = 1 (ν_{24})	18222.55	6359.41	4868.95	-0.7768
v = 1 (ν_{23})	18301.52	6331.44	4861.80	-0.7813
v = 1 (ν_{16})	18391.85	6361.68	4850.46	-0.7768

		A-C	κ
v = 2 (ν_{24})		13356.0	-0.7803
v = 2 (ν_{23})	"A"	13522.0	-0.7897
	"E"	13519.2	-0.7897

CD_3OCHCH_2

	A	B	C	κ
v = 0	15833.39	5697.45	4425.15	-0.7770
v = 1 (ν_{16})	15860.40	5662.93	4410.48	-0.7812

found from this microwave work have been designated ν_{23}, ν_{24}, and ν_{16} on the assumption that they represent, respectively, the two lowest out-of-plane vibrations and the lowest in-plane vibration of the molecule. Careful studies at low pressures showed that the microwave lines corresponding to v = 1 (ν_{23}) were broader than the others, and for two transitions ($7_{25} - 7_{16}$ and $8_{26} - 8_{17}$) the lines were in fact resolved into doublets. Thus the ν_{23} vibration corresponds to the torsional motion of the methyl top. Microwave lines have also been assigned to the v = 2 (ν_{24}), v = 2 (ν_{16}), and v = 2 (ν_{23}) states, and although no splittings were found in the first two, the lines of v = 2 (ν_{23}) occurred as A and E doublets separated by a few megacycles. Table IX shows the values computed for the barrier to internal rotation of the methyl top from data obtained from different sources. The most accurate value, which is taken from the splitting of the A and E levels of the v = 2 state, is unusually high, 3820 ± 100 cal/mole. A possibly important contribution to this barrier comes from steric interaction of the methyl group with the vinyl hydrogen atoms. The minimum H-H distance in the cis conformation of the structure as proposed in Fig. 11 is about 1.6Å.

TABLE IX

Barrier to Internal Rotation in cis Methyl Vinyl Ether.

From $\Delta\nu$ of v = 2	V_3 = 3830 ± 100 cal/mole
From $\Delta\nu$ of v = 1	V_3 = 3750 ± 100 cal/mole
From Raman Line at 240 ± 10 cm^{-1}	V_3 = 3930 ± 350 cal/mole
From Relative Intensity of Microwave Lines	V_3 = 3430 ± 450 cal/mole
Final Value	V_3 = 3830 ± 100 cal/mole

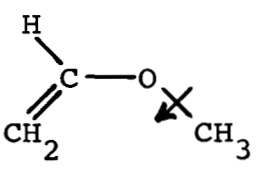

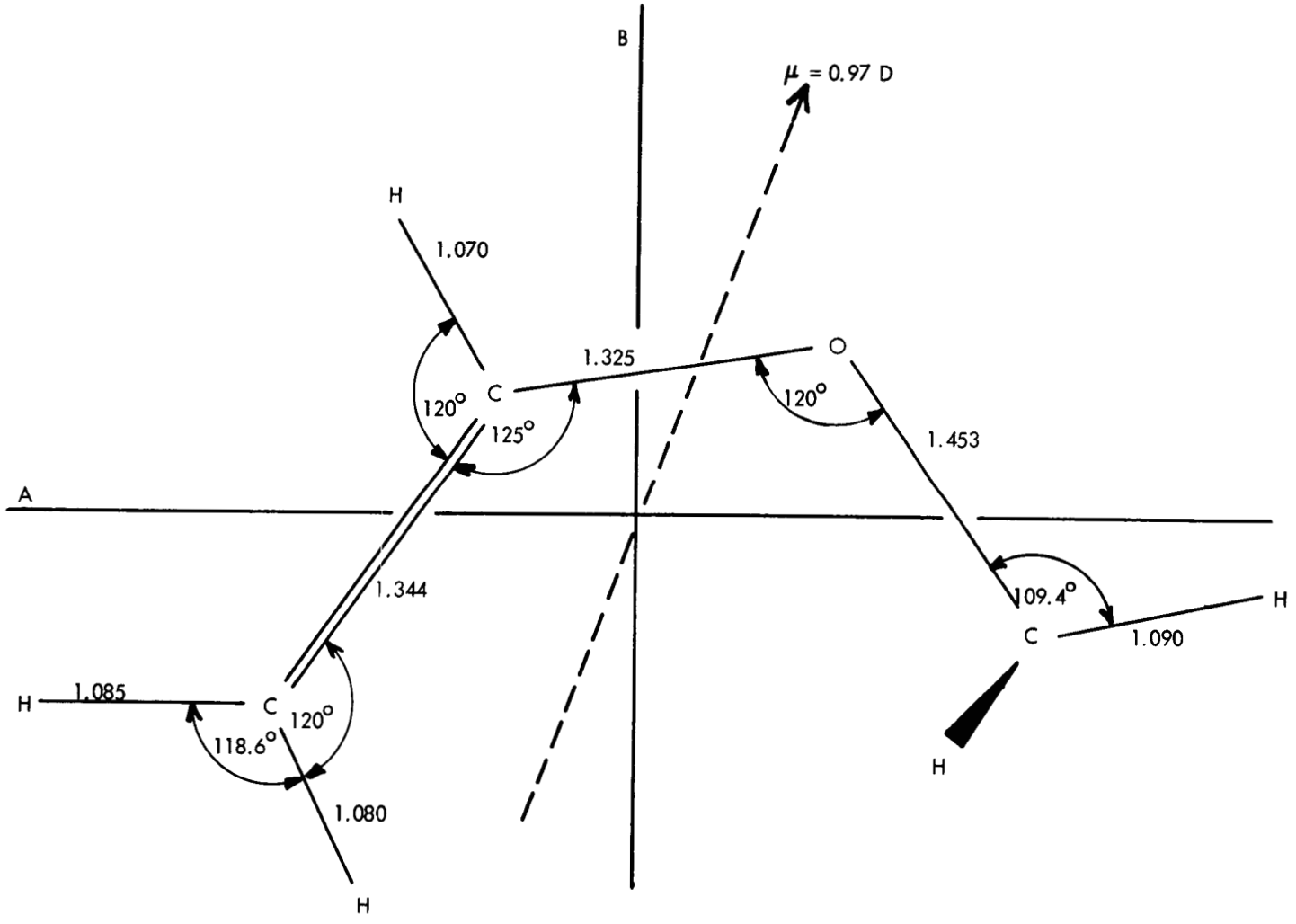

Fig. 11 Approximate structure of cis methyl vinyl ether.

TABLE X

Low-Frequency Vibrations of cis Methyl Vinyl Ether

	$\nu_{24}(cm^{-1})$	$\nu_{23}(cm^{-1})$	$\nu_{16}(cm^{-1})$
Microwave Spectra (relative intensity)	219 ± 20	225 ± 10	310 ± 20
Far Infrared Spectra (Vapor)		230 (broad)*	328 ± J
Raman Spectra (solution)	205 ± 15	240 ± 10	327 ± 2

	Probable Assignment
ν_{24}	torsion about C-O bond
ν_{23}	torsion about CH_3 group
ν_{16}	in-plane skeletal bending of C-O-C group

*Evident structure showing two possible bond centers at 228 and 216 cm^{-1}.

This is considerably less than the sum of the van der Waals radii for the two hydrogen atoms (2.4Å). For the molecule methyl formate, with a methyl top barrier of 1190 cal/mole, the analogous O-H distance of nearest approach is 2.15Å, while the sum of the van der Waals radii concerned is 2.6Å. In this instance, however, the interaction is attractive as compared with repulsive for methyl vinyl ether.

In Table X the values for the vibrational frequencies are listed as determined from different sources. Raman and far infrared spectra were taken in order to confirm the microwave data, and their results agree quite well. The far infrared spectrum of the vapor was taken at Princeton University on a Beckman spectrograph through the courtesy of Professor George Leroi.

Program for the next interval: A search in the 35- to 50-Gc spectral region will be made on the deuterated species with the hope of observing the second rotational isomer. The above work will be prepared for publication.

*This research was also supported in part by the Air Force Office of Scientific Research under Grant AF-AFOSR-330-63, and in part by the Office of Naval Research under Contract Nonr-266(45).

(1) W. Klemperer, private communication.

C. SCATTERING OF VELOCITY SELECTED MOLECULAR BEAMS*

(P. Cahill, M. Hessel, P. Kusch, and S. Skwire)

The molecular beam velocity selector has been reconditioned. Measurements will be made of the absolute scattering cross section of K on Ar and of KCl on Ar and N_2. A refrigerated McLeod gauge[1] will be used as the primary standard for calibration of the ion gauge.

*This research was also supported in part by the Air Force Office of Scientific Research under Grant AF-AFOSR-330-63, and in part by the Office of Naval Research under Contract Nonr-266(45).

(1) E. W. Rothe, J. Vac. Soc. 1, 66 (1964).

D. MAGNETIC ROTATION SPECTRA*

(P. Kusch, B. Palatnick)

A magnetic rotation spectrum of CS_2 has been previously observed in the spectral region 3640-3125Å.[1] Recently the spectrum has been extended to about 2930Å on the low-wavelength side of the spectrum and to about 3775Å on the high-wavelength side. In addition, new spectral lines have been found in the previously studied region.

The new lines at high wavelengths were brought out by increasing the sample pressure to 28 cm of Hg, which is the vapor pressure of CS_2 at room temperature. This is roughly 10 times the pressures previously employed in the experiment. At such high pressures, the lines at lower wavelengths tend to disappear because of absorption.

Recent exposures have been made on Kodak 103a-0 photographic plates. Work is in progress on the reduction and analysis of data.

Program for the next interval: Work will continue on the reduction and analysis of data.

*This research was also supported in part by the Air Force Office of Scientific Research under Grant AF-AFOSR-330-63, and in part by the Office of Naval Research under Contract Nonr-266(45).

(1) P. Kusch and F. W. Loomis, Phys. Rev. 55, 850 (1939).

E. MOLECULAR SPECTRA OF CESIUM*

(M. Hessel, P. Kusch)

In the 1930's Kusch and Loomis[1] investigated the absorption spectrum of molecular cesium, Cs_2. Measurements were made of five distinct band systems whose maxima occurred at 4800Å, 6250Å, 7200Å, 7667Å, and 8950Å. A reasonably complete vibrational analysis of the 7667Å system was given, but several of the other systems have been only partially analyzed. The 7667Å system extends to very high vibrational quantum numbers v" and v' of 50 to 65, where v" is the vibrational quantum number of the ground state and v' that of the excited electronic state. A reanalysis of the existing data for the 7667Å system, not all of which had entered into the earlier assignment, indicates that there are almost certainly perturbations of the vibrational states of the excited electronic state. To proceed any further on this problem, spectrographic plates of the absorption spectra of molecular cesium at high resolution and high dispersion must be obtained.

A program to supply the needed spectrographic data for Cs_2 has been undertaken. Figure 12 is a diagram of the experimental arrangement. A 90-cm-long 7.5-cm-diameter glass absorption tube (B) was baked out to 400°C and filled at a pressure of 5×10^{-8} Torr with approximately one gram of 99.9% pure cesium. The absorption tube was placed inside a brass oven (C) and heated to temperatures between room temperature and 450°C by means of a Nichrome coil (E) that was wound around the whole length of the brass oven. There were closer windings near the ends at the aluminum cap to keep the window hotter than the rest of the cell and therefore free of condensed cesium. Preliminary experiments

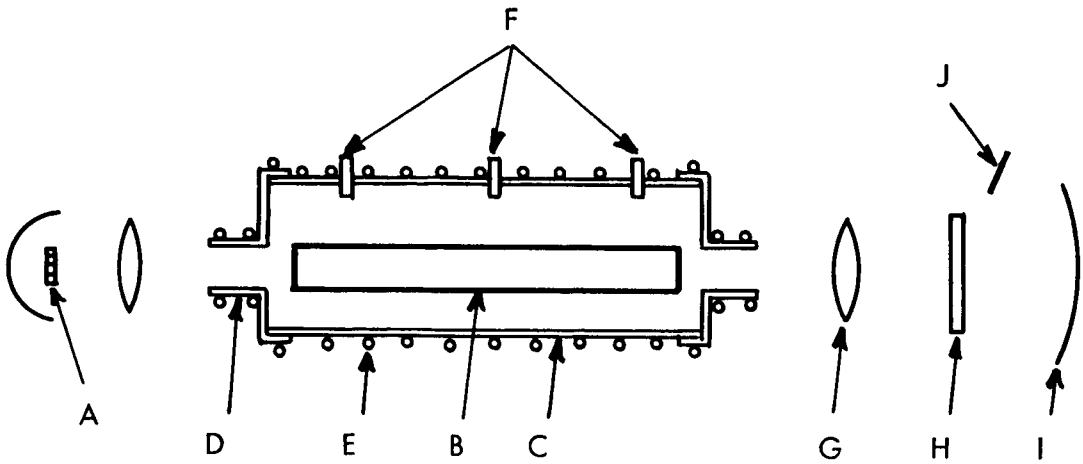

A Tungsten-Iodine Light Source
B 7052 Glass Absorption Cell
C Brass Tube Oven
D Aluminum End Cap
E Nichrome Heating Wire
F Thermocouple Well
G Lens
H Filter
I Concave Grating
J Photographic Plate

Fig. 12 Schematic diagram of apparatus.

were made with Pyrex absorption tubes. The cesium rapidly reacted with the glass at temperatures above 300°C, and the cell lasted for only 1 to 2 hours. 7052 Corning glass was found to be satisfactory at temperatures below 400°C. The cells lasted for 100 hours. Preliminary data have been taken on a low dispersion 5.5 Å/mm 3-meter Baird concave-grating spectrograph. All the band systems mentioned above were observed, and in addition it was found that the 8950Å band system extends to at least 11,500Å.

The band spectra of Cs_2 are interesting because of the very large number of vibrational states that appear, and a very high resolution spectrograph is required to resolve vibrational structure. No spectrographic equipment with suitably high resolution and high dispersion was available at Columbia University or its environs. Dr. Mark Fred of the Chemistry Division of Argonne National Laboratory has kindly permitted us to use the Argonne 30-foot concave-grating spectrograph.[2] It has a resolution of about 90,000 and a dispersion of 1.8 Å/mm in the first order. We have photographed the absorption spectra of Cs_2 in three orders at a range of experimental conditions from 24°C to 450°C and exposure time to develop the maximum possible information.

Program for the next interval: To determine the wavelength of the spectra and obtain microphotometer traces. Additional exposures will probably have to be taken as the analysis of the spectra proceeds.

*This research was also supported in part by the Air Force Office of Scientific Research under Grant AF-AFOSR-330-63, and in part by the Office of Naval Research under Contract Nonr-266(45).

(1) F. W. Loomis and P. Kusch, Phys. Rev. 46, 292 (1934).
(2) F. S. Tomkins and M. Fred, Spectrochim. Acta. 6, 139 (1954).

IV. SOLID STATE PHYSICS

A. INTERACTION BETWEEN A NEUTRAL BEAM AND A CONDUCTING SURFACE* (P. Kusch, D. Raskin)

The experimental problem in this research is to measure the ratio of the intensity of a sharply defined molecular beam in the geometrical shadow of an obstacle in the beam to the intensity of the beam outside of the shadow. The data are to be interpreted as indicative of the interaction of the electric dipole moment of a molecule with its image in the obstacle. A number of effects that give rise to an intensity in the shadow can occur, and it is essential to identify and exclude such effects.

In the previous report it was stated that measured relative beam intensities as defined above were four times as high as the theoretical prediction. In addition, the intensities decreased as the pressure in the vacuum chamber decreased. A plot of the logarithm of relative intensity vs pressure was linear for each point in the shadow of the obstacle, and the data could be extrapolated to zero pressure. The extrapolated intensities were about twice as high as expected on the basis of a preliminary model of the interaction process.

An attempt was made to determine what effect heating the conducting surface had on the beam profile in the shadow. While beam intensities were measured, the surface was heated moderately (to 200°C).

With the surface hot, the intensities no longer showed a pressure dependence. In addition, the relative intensities decreased to within 20% of the theoretical expectation. The

physical mechanism for the temperature and pressure dependence is still unexplained. It is difficult to interpret the result as a scattering process in the residual gas in the apparatus. The two bodies of data are clearly not consistent.

Since the pressure dependence does not appear to be present when the surface is heated, and since it appears to be feasible to extrapolate to zero pressure if a pressure effect occurs, it does not seem worthwhile at present to make the large investment in an ultrahigh vacuum system that had previously been contemplated. It may still be necessary to build a new vacuum system, but this step will not be taken until the effect of pressure has been studied further.

The measured beam profile is now in fairly close agreement with the theory. There is no significant doubt that the effect in question, never before observed, has in fact now been observed. However, the "discontinuity" in the beam profile at the beginning of the geometrical shadow is not as sharp as it should be according to simple calculations. This probably indicates that the two 10μ slits, one to define the beam and the other to select a portion of the final beam for detection, and the edge of the conducting cylinder are not aligned perfectly parallel to each other. The ability to locate the edge of the shadow precisely is important to the experiment; therefore, the alignment will have to be improved.

Program for the next interval: All the components that define the beam (slits, cylinder, and detection unit) will be mounted on a rigid bench that can be removed as a unit from the vacuum system. The alignment of these pieces will be done with the bench outside the system. This will allow for greater ease

and accuracy in making the adjustments. A method has been devised for attaching straight-edged sections to the slits and cylinder in such a way that the straight-edge is accurately parallel to the piece in question. This will extend the effective height of the piece to make alignment with a telescope cross-hair more accurate.

The components for the bench have been designed and will be constructed shortly. Once the bench is assembled and tested and the parts are aligned, the behavior of the beam profile with temperature and pressure variation will be studied.

The following experiments will then be performed: (1) To determine the dependence of the beam profile on the cylinder radius; (2) To observe the difference in beam profile when a dielectric cylinder is put in place of the conducting surface; (3) To ascertain the extent by which an atomic beam is deflected by the surface.

*This research was also supported by the Army Research Office (Durham) under Grant DA-ARO(D)-31-124-G568.

B. ADIABATIC DEMAGNETIZATION IN THE ROTATING FRAME*

(H. Einbinder, S. R. Hartmann)

The receiver for nuclear signals mentioned in the last Quarterly Progress Report[1] was completed. A series of experiments were performed to determine the effects of irradiating the F^{19} spin system in CaF_2 with a radio-frequency magnetic field of magnitude comparable with the field due to neighboring nuclei in the specimen. The spin system was adiabatically demagnetized in the rotating frame before irradiation. A considerable amount of data was taken and is now being processed.

Program for the next interval: Analysis of the data obtained this quarter will be completed, and a theoretical explanation of the effects observed will be attempted.

*This research was also supported by the National Science Foundation under Grant NSF-GP 3379.

(1) CRL Quarterly Progress Report, June 15, 1965, p. 31.

C. HIGH-FREQUENCY PROPERTIES OF SUPERCONDUCTORS*
(S. Zemon)

A paper describing the research on zinc has been prepared for publication.

Due to a change in personnel, this program will be temporarily suspended.

*This research was also supported in part by the National Science Foundation under Grants NSF-GP 1031 and NSF-GP 4324 and in part by the Office of Naval Research under Contract Nonr-3994(00).

D. ELECTRONIC TUNNELING IN THE SUPERCONDUCTING STATE*
(S. Zemon)

Work proceeded on this project for only one month in this quarter. During that time several junctions of aluminum-aluminum, zinc-aluminum, and cadmium-aluminum were tested, and all were unsatisfactory. Current-voltage curves characteristic of high-resistance shorts between the films were observed. The trouble is probably due to the presence of pin holes in the aluminum oxide layer. This difficulty cannot be reliably overcome without having more control over the evaporation procedure than is now available.

The following improvements were made. Adhesion of zinc and cadmium films to the substrate was increased by depositing an aluminum underlayer first. An arrangement was contrived for bringing the films outside the microwave cavity and for establishing electrical contact with copper electrodes glued to the substrate.

Due to a change in personnel, this program will be temporarily suspended.

*This research was also supported in part by the National Science Foundation under Grants NSF-GP 1031 and NSF-GP 4324 and in part by the Office of Naval Research under Contract Nonr-3994(00).

E. NUCLEAR MAGNETIC RESONANCE IN PLATINUM*

(S. R. Hartmann, G. R. Mather)

Efforts to find the platinum resonance in the fine ($\approx$50Å dimension) particles have been unsuccessful to date.

After preparing a sample of 0.1 gram of 10-μ platinum particles mixed in 2 grams of sulphur and observing a signal-to-noise ratio of about three at the receiver video output,[1] another sample, also similar to the 50Å particle sample, was prepared as follows: 0.1 gram of the 10-μ particles was thoroughly mixed with 2 grams of the fine particle sample (5% Pt on carbon); this mixture was then placed in a container and coil similar to those used previously. Again, a definite platinum resonance was observed at a temperature of 1.5°K, thereby indicating that the carbon on which the fine particles are deposited does not short out the rf pulses and signal.

It was found that another kind of fine particle sample is readily available commercially. This is platinum black, and it consists of platinum in crystallite sizes of about 100Å; because

of agglomeration of these crystals due to electrostatic attraction, however, the particle sizes are at best uncertain. A sample consisting of 2.5 grams of platinum black mixed in vaseline was prepared and the resonance sought at temperatures of 1.5°K and 4.2°K; again, no resonance was found.

The fact that abundance of platinum presents no signal-to-noise problems in the platinum black indicates that there must be other reasons for the absence of the resonance. Charles and Harrison[2] note that extensive inhomogenious broadening of the resonance line can occur in particles which are fine enough for surface effects to play an important role. Undoubtedly, this broadening is present in our platinum sample, and it is possible that it may in some way be preventing observation of the resonance.

Program for the next interval: We shall continue to look for the resonance in the platinum black sample. Should all attempts fail, we will procure platinum samples in particle sizes between 100Å and 10μ, where the resonance has already been observed.

*This research was also supported by the National Science Foundation under Grant NSF-GP 3379.

(1) CRL Quarterly Progress Report, June 15, 1965, p. 33.
(2) R. J. Charles and W. A. Harrison, Phys. Rev. Letters 11, 75 (1963).

V. OPTICAL AND MICROWAVE MASERS

A. INFRARED AND OPTICAL MASERS

1. Optical Maser Spectroscopy

a. Light-Scattering Homodyne Spectroscopy*

(S. S. Alpert, D. A. Balzarini, L. Seigel, L. R. Wilcox, and Y. Yeh)

Introduction. The work undertaken during this quarter was concerned primarily with a systematic study of the scattered light spectrum of carbon dioxide maintained near the critical point. A He-Ne laser homodyne spectrometer as described in previous Quarterly Progress Reports and in the literature[1,2,3] was used to observe the spectral profile of the scattered light as a function of both scattering angle and temperature. Further experimentation has successfully shown the feasibility of modifying the optical system of the laser homodyne spectrometer so as to obviate inaccuracies in determining the angle of scatter. This point will be further discussed in this report.

[1] Carbon Dioxide Scattering Observations. Observation was made of the central unshifted line of the scattered light spectrum of carbon dioxide. This was done using the He-Ne laser homodyne spectrometer developed by Cummins, Knable, and Yeh.[3]

The spectral distribution of the light scattered by the carbon dioxide near its critical point was found to be strongly temperature sensitive. The observed profiles were approximately Lorentzian in shape, and the half-width was observed to vary linearly with temperature in the neighborhood of the critical temperature (Fig. 13). The slope of the temperature plot is 4.6 ± 1.0 kc/sec/°C and the intercept is 92 cps. The intercept is about six times the instrumental resolution (15 cps).

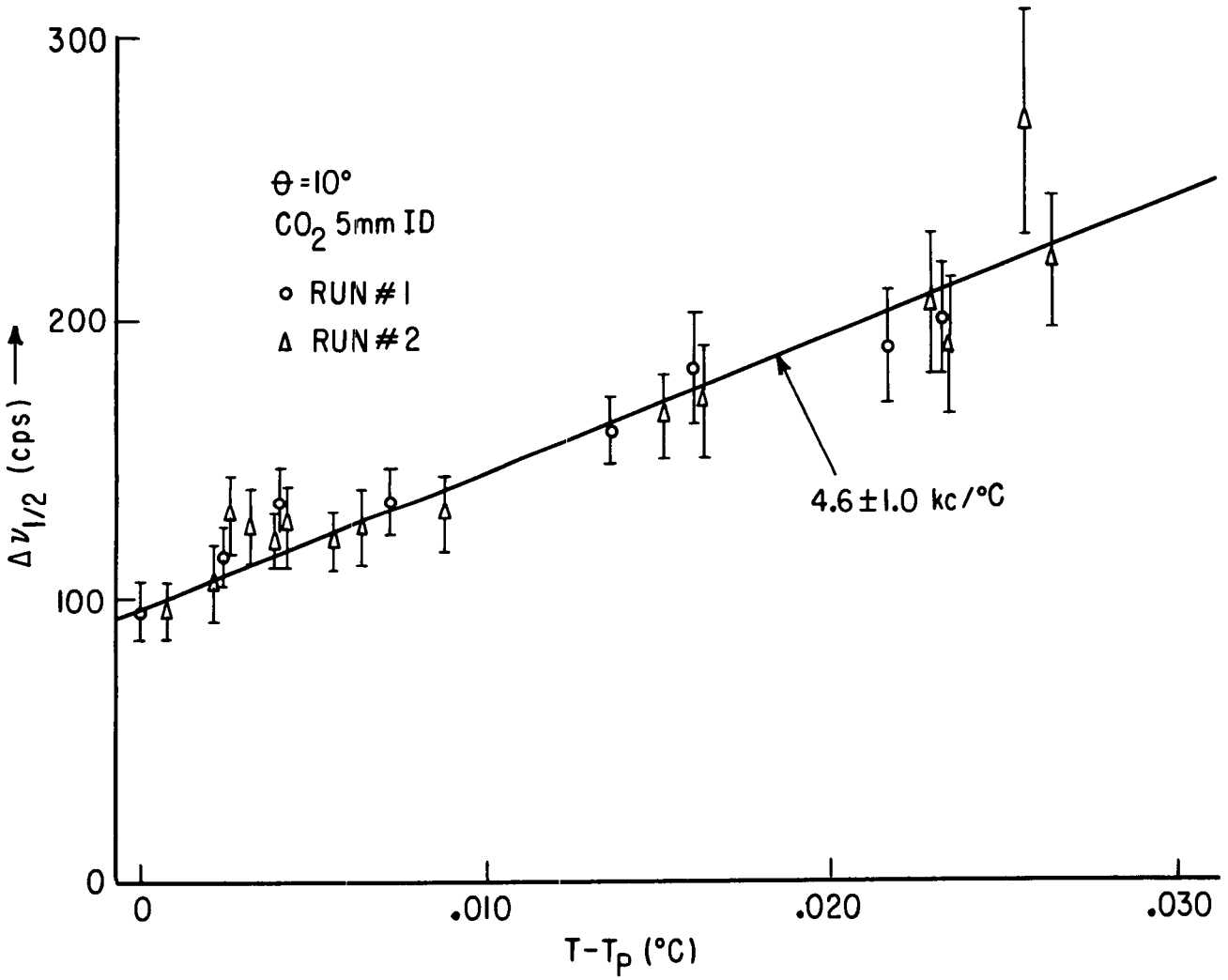

Fig. 13 The full spectral half-width vs the temperature T relative to the phase separation temperature T_p.

The spectrum of the scattered light was studied over a range of scattering angles (θ) at a fixed temperature (Fig. 14). The width of the Lorentzian profile varied linearly with $\sin^2(\theta/2)$. The intercept of the angular plot, (Fig. 14), is about 40 cps and is believed to result from the finite resolution of the spectrometer (15 cps), from the finite angular aperture of the optical system, and from small errors in determining the scattering angle (θ).

The results obtained in this experiment can be interpreted on the basis of the classical scattering theory of Mountain,[4] which follows closely that of Landau and Placzek.[5] Using a hydrodynamical theory of fluctuations, Mountain[4] has shown that the central component of the light scattered from a pure single-phase fluid has the form $\sigma(\vec{k},\nu)$.

$$\sigma(\vec{k},\nu) = \frac{c_p - c_v}{c_p} \frac{\Lambda k^2/(\pi\rho_o c_p)}{[\Lambda k^2/(2\pi\rho_o c_p)]^2 + \nu^2} , \qquad (1)$$

where $\vec{k}$ is the change in the propagation vector of the scattered light relative to that of the incident light, ν is the frequency shift of the scattered light relative to the frequency of the incident light, c_p and c_v are the specific heat capacities at constant pressure and volume respectively, Λ is the thermal conductivity, and ρ_o is the mean density of the material. It is readily seen from Eq. (1) that the expected spectral profile is Lorentzian. The change in the propagation vector $\vec{k}$ is given by

$$|\vec{k}| = \frac{4\pi}{\lambda} \sin(\theta/2) , \qquad (2)$$

where λ is the wavelength of the incident light in the medium and where θ is the scattering angle. Substitution of Eq. (2) into

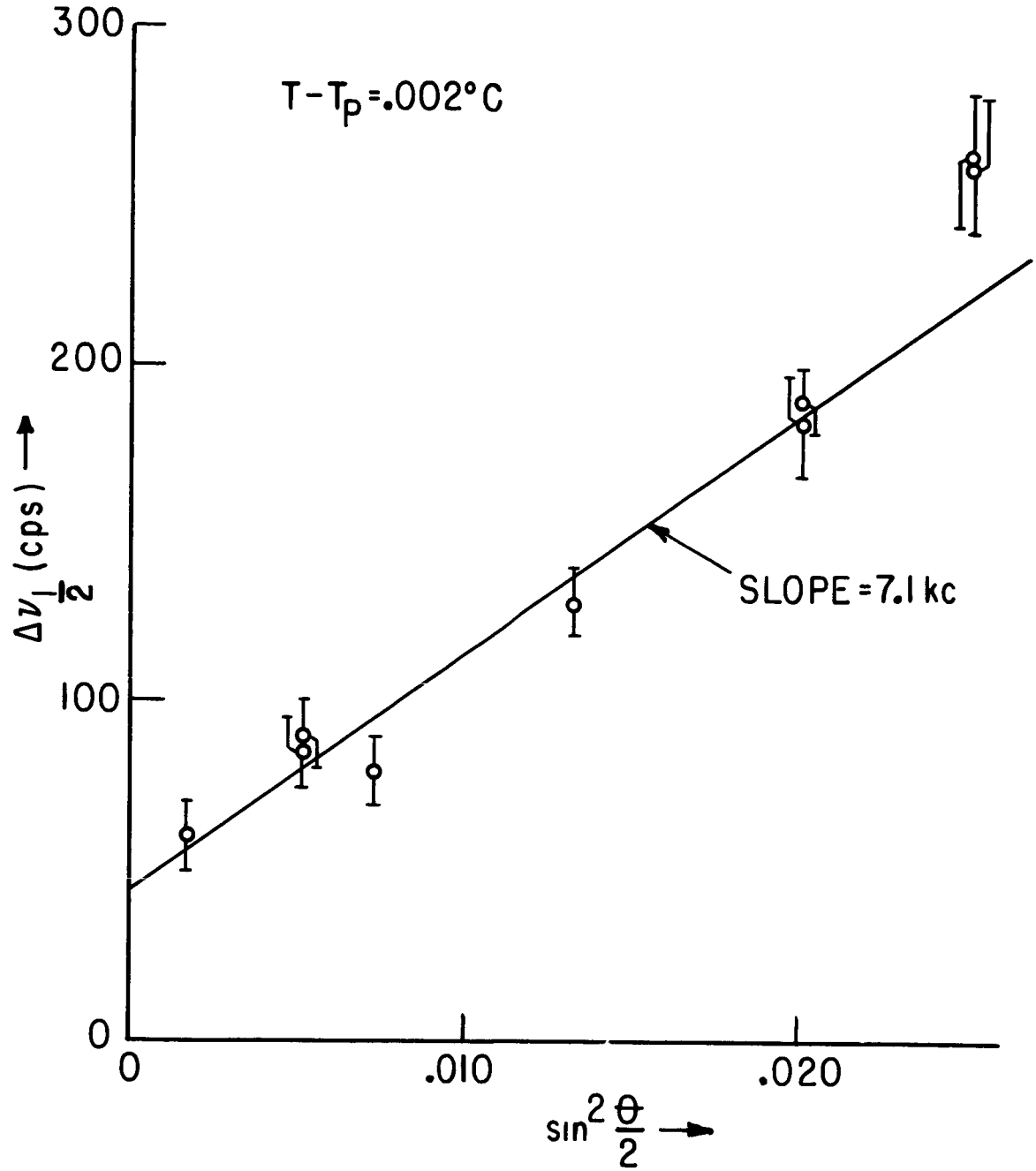

Fig. 14 The full spectral half-width vs $\sin^2(\theta/2)$.

Experimentation has shown that the collection lens can be omitted, resulting in the optical geometry shown in Fig. 15. The arrangement shown in Fig. 15 gives satisfactory results, defines the angular precision by the angular spread of the scattered light onto the masked beam splitter ($\pm\frac{1}{6}^{\circ}$), and reduces "shot" noise in the detecting photomultiplier by eliminating much light which does not contribute to the desired signal.

Program for the next interval. 1. The signal-to-noise ratio is known to be proportional to the energy falling on the scattering cell. At present only 1 to 2 mW of 6328Å light in the fundamental laser mode falls onto the scattering cell. A Spectra Physics, Model 125, He-Ne laser has been purchased. This stable laser has a power output of 50-70 mW in the fundamental mode. The use of this high-powered laser should increase the signal-to-noise ratio by a factor of from 25 to 50.

2. The laser homodyne spectrometer is essentially a Mach-Zender interferometer. Operating in each "leg" of this interferometer is a Bragg tank[6] modulator, the purpose of which is to step up the light frequency by a known amount. The "beat" frequency between the two optical "legs" is then detected. The Bragg tank modulators are at best about 30% efficient, i.e., 30% of the incident light is single-sideband modulated. Direct elimination of one Bragg tank would deliver more light to the scattering cell but would also result in electronic problems of radio-frequency pickup. An attempt is now being made to: (a) make the Bragg tanks more efficient light modulators by driving them harder, and (b) to shield the tanks more satisfactorily so that one might be eliminated.

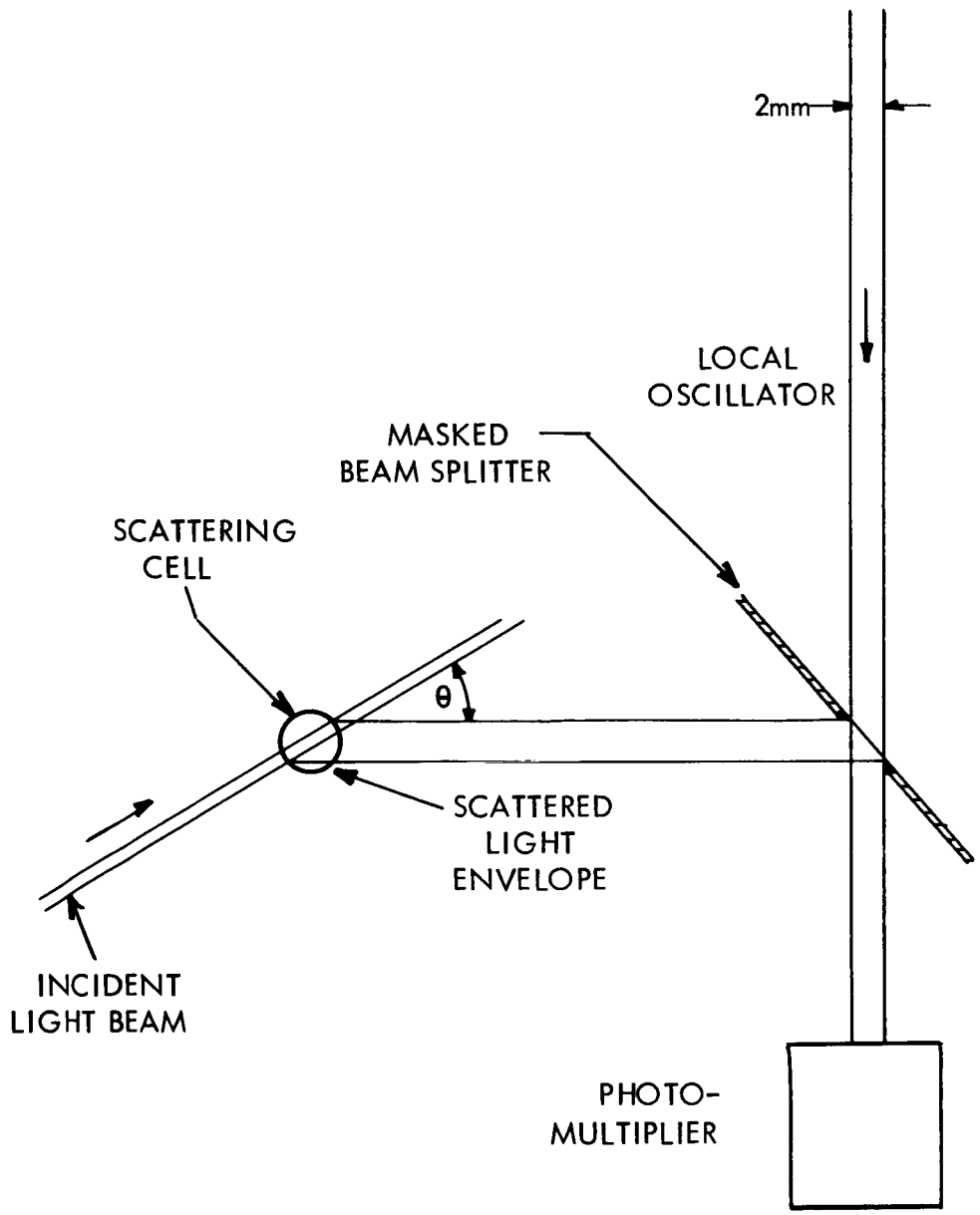

Fig. 15 Lensless scattering geometry. Note that there is no collecting lens.

*This research was also supported by the Army Research Office under Contract DA-31-124-ARO-D-296.

(1) CRL Quarterly Progress Report, June 15, 1963, p. 35.
(2) CRL Quarterly Progress Report, December 15, 1963, p. 45.
(3) H. Z. Cummins, N. Knable, and Y. Yeh, Phys. Rev. Letters 12, 150 (1964).
(4) R. Mountain, Rev. Mod. Phys. (to be published).
(5) L. D. Landau and G. Placzek, Physik Z. Soviet Union 5, 172 (1934).
(6) H. Z. Cummins and N. Knable, Proc. IEEE 51, 1246 (1963).

---

b. Laser Studies of Molecular Birefringence*

[1] Birefringence Induced in Fluids by an Inhomogeneous Electric Field.
(R. L. Disch, S. Golub)

(a) Direct Measurement of the Quadrupole Polarizability of the CCl_4 Molecule. A uniform electric field induces a dipole moment in an atom or molecule; for spherical or "quasi-spherical" molecules, the induced dipole moment is given by

$$m = \alpha F \ ,$$

where α is the electric polarizability. In addition, the electric field induces a quadrupole moment in the molecule. For "quasi-spherical" systems this is proportional to the square of the electric-field strength:

$$Q = \frac{1}{2} BF^2 \ .$$

Q, the induced quadrupole moment, is defined by

$$Q = \frac{1}{2} \sum_i e_i r_i^2 (3\cos^2\theta - 1) \ ,$$

in the usual notation.

Little is known concerning the so-called "quadrupole polarizability" B. It has been calculated exactly for the hydrogen atom,[1,2] a system for which the Schrödinger equation may be solved to any desired order of the electric field. For the ground state, B was found to have the value -0.487×10^{-38} esu. No exact theoretical values are known for other systems, and there existed heretofore no experimental values of this molecular property.

The quadrupole polarizability should be directly measurable by observing the birefringence induced in a fluid of quasi-spherical molecules by an inhomogeneous electric field.[3] However, this effect is extremely feeble, so a substance known to have a rather high dipole polarizability, CCl_4, was chosen for the initial search. It was studied in the liquid phase at room temperature. The preliminary value of B obtained in this experiment is

$$B_{CCl_4} = -1.26 \times 10^{-38} \text{ esu.}$$

This value of B is only about 2.5 times that of the hydrogen atom, a ratio considerably smaller than the ratio of their dipole polarizabilities. An approximate theoretical value of B for the helium atom can be obtained by the screening approximation.[4] The result is $B_{He} = -0.0271 \times 10^{-38}$ esu. Here, by contrast, the ratio B_{CCl_4}/B_{He} is considerably greater than the ratio of the dipole polarizabilities.

Program for the next interval: Refinement of measurements of nonquadrupolar molecules and studies of the thermal dependence of the birefringence induced by an inhomogeneous electric field in order to obtain better values of both the permanent molecular

quadrupole moment and the quadrupole polarizability. The possibility of using an even more intense light source and higher applied field gradients is being investigated.

[2] A Laser Polarimeter
(R. L. Disch, J. Matuska, D. Sverdlik)

Construction of the ultra-sensitive polarimeter discussed in the previous Quarterly Progress Report is nearing completion. This will be used in several investigations, one of which is briefly discussed below.

[3] The Anisotropy of Molecular Optical Activity
(R. L. Disch, D. Sverdlik)

A theoretical investigation has been made concerning the possibility of effecting a drastic improvement in signal-to-noise ratios in the study of the optical activity of partially oriented systems. The only previous attempt at such measurements is that of Tinoco.[5,6] An improvement which can increase signal-to-noise ratios by a factor of 100 at the expense of greater experimental complexity has been thoroughly studied, and it is concluded that an attempt to attain this improvement is worthwhile. Details of this method will be given in a later report.

*This research was also supported by the Army Research Office under Contract DA-31-124-ARO-D-305.

(1) Buckingham, Coulson, and Lewis, Proc. Phys. Soc. (London) A69, 639 (1956).
(2) Coulson and Stephen, Proc. Phys. Soc. (London) A69, 777 (1956).
(3) Buckingham, J. Chem. Phys. 30, 1580 (1959).
(4) Disch, et al., to be published.
(5) Tinoco and Hammerle, J. Am. Chem. Soc. 60, 1619 (1956).
(6) Tinoco, J. Am. Chem. Soc. 81, 1540 (1959).

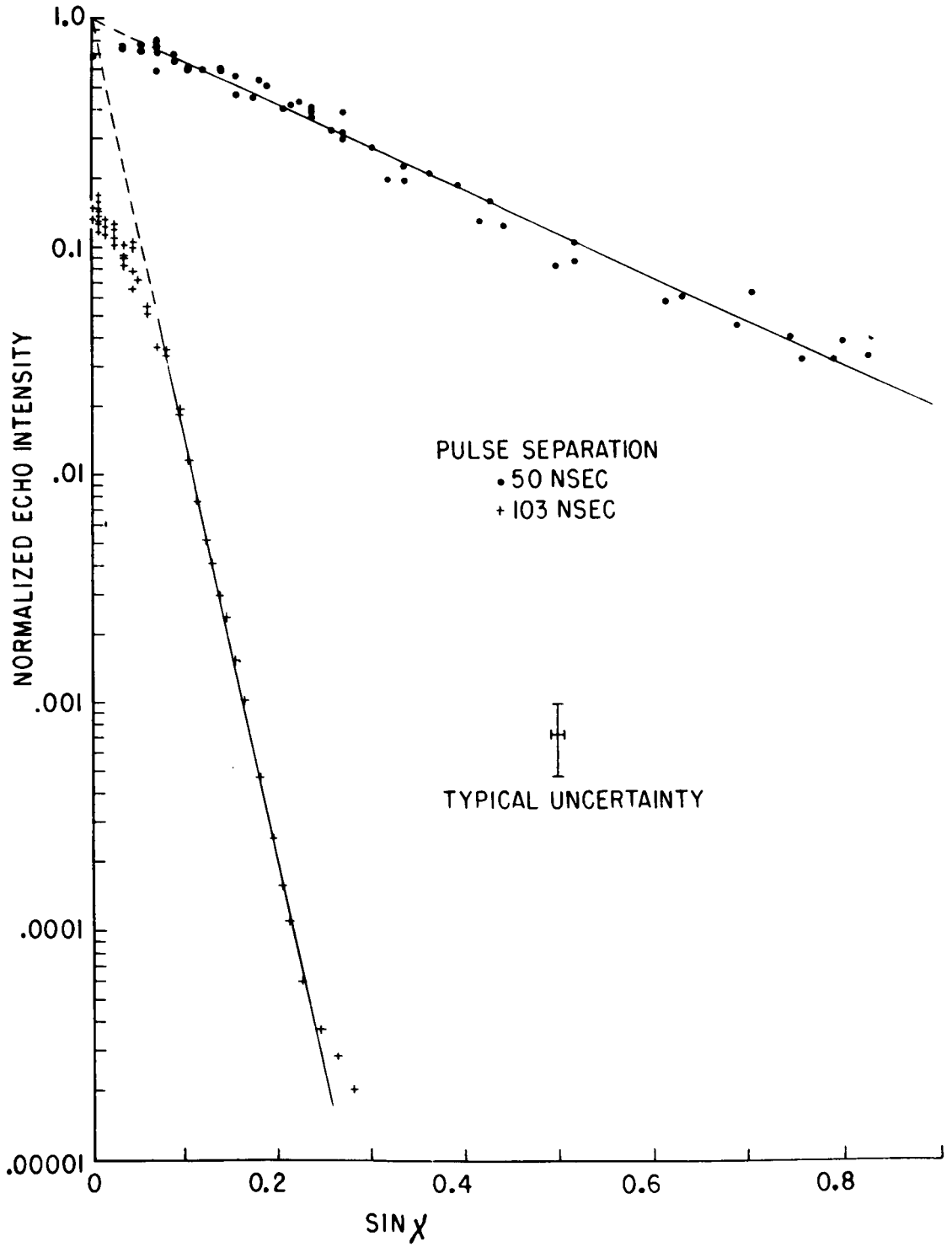

Fig. 16 Echo dependence on angular direction of magnetic field with respect to optic axis of sample for different values of τ_s. Each set of data is separately normalized.

2. Ruby Laser: Photon-Echo Resonance*
(I. D. Abella, S. R. Hartmann, N. A. Kurnit)

Measurements of the photon echo intensity, as a function of the angle, χ, between the optic axis of the ruby sample and the magnetic field, were repeated after it was found that the photomultiplier used as a detector was saturating at the higher signal intensities. Results reported previously[1] remain unchanged in broad outline, but are not correct in specific details. The functional dependence of the echo intensity on magnetic field angle appears closer to exponential than Gaussian, as indicated in Fig. 16, except at angles so small that optic-axis wandering and correct alignment may become critical. The relationship, $\Delta\chi_{1/2}\tau_s^2$ = constant, found previously does not seem to hold true, but there is, as yet, insufficient data to obtain a more accurate expression.

Program for the next interval: Further measurements of the temperature and magnetic field dependence of the photon echo will be made after a system for electronic processing of the data is completed.

*This research was also supported by the Army Research Office under Contracts DA-31-124-ARO-D-224 and DA-31-124-ARO-D-341.

(1) CRL Quarterly Progress Report, March 15, 1965, p. 52.

B. RUBIDIUM MASER*
(P. Davidovits, W. Happer, E. B. Saloman, W. A. Stern)

Publications are being prepared to cover the research that has been done in this field. Because of a change in personnel, work on this project has temporarily been halted. Further work will be undertaken with the initial goal of observing

modulation of the pumping light at the microwave frequency of the maser transition. There is some question as to how the modulation of the light actually depends on the spectral profile of the pumping lamp. This modulation effect could provide a convenient way of keeping the maser cavity tuned. Thus, this effect is of interest both in determining fundamental physical properties and in improving the operation of the rubidium maser.

*This research was also supported by the Office of Naval Research under Contract Nonr-4259(10).

VI. RADIOASTRONOMY

A. MODELS OF PLANETARY ATMOSPHERES*

(W. Ho, I. Kaufman, P. Thaddeus†)

The microwave cavity spectrometer has been modified to permit measurement of microwave absorption in gas mixtures containing water vapor. The major modifications have been designed to prevent condensation of water vapor in the gas-filled parts of the system during the period of a series of measurements. Comparison among the various methods of measuring the density of water vapor in the cavity has shown that determination of the shift in resonant frequency when the water vapor is admitted is more accurate than measurement of either the temperature of the liquid water reservoir in contact with the vapor in the cavity or the change in cavity length required to keep the resonant frequency constant.

Preliminary measurements have been made at 9260 Mc/sec and 120°C on mixtures of water vapor at 100, 300, 500, and 700 mm of mercury partial pressure and nitrogen at a total pressure of 120 atmospheres. The absorption is large enough to be observed with the present apparatus.

A microwave cavity has been constructed which will enable measurements to be made of microwave absorption at gas pressures as high as 500 atm. This cavity is a cylinder 1/4 inch in diameter and 20 inches long, which passes through a series of TE_{11n}-mode resonances at 35,000 Mc/sec as the gas pressure is varied from zero up to the maximum.

The cavity and associated hardware to compress the gas and fill the cavity have been constructed, assembled, and pressure tested. Resonances have been observed and identified, and the techniques and equipment needed to measure the cavity Q are currently being developed.

Program for the next interval: Analysis of the measurements of nonresonant absorption by mixtures of carbon dioxide and nitrogen, and carbon dioxide and argon, and their application to the study of the atmosphere of Venus will continue.

*This research was also supported by the National Aeronautics and Space Administration under Grant NsG-442.

†NASA Institute for Space Studies.

VII. X-RAY ASTRONOMY

A. POLARIZATION MEASUREMENTS

(R. C. Isler, A. Lurio, R. Novick, F. Kantor, and T. Wing)

Difficulties associated with using liquid hydrogen as a scatterer of cosmic x rays have led to investigation of using a lithium or lithium-hydride scatterer to make a polarization measurement. Due to the higher absorption in these materials of soft x rays, the polarization measurement would be made in the 15-50 keV region. At least one source, the Crab nebula, has a significant flux in this range.(1)

The design being considered consists of alternate rows of lithium scatterer and proportional counters extending the 5-ft length of the rocket apparatus compartment. The rows of lithium will be divided into segments by equally spaced thin sheets of steel placed perpendicular to the length of each row, which will be opaque to the x rays. The measurement will be made with the rocket spinning in a plane perpendicular to the flux, keeping the same side of the rocket pointed toward the source.

Computations have been made of the apparent polarization of a completely polarized source and of the efficiency of a rectangular block as a scatterer. The computations have been checked by measurements.

The apparent polarization of a completely polarized source is defined as:

$$P_m = \frac{P_1 - P_2}{P_1 + P_2} ,$$

where P_1 is the counting rate with the rows of lithium parallel to the polarization vector, and P_2 is the counting rate with the

rows perpendicular to the polarization vector. P_m is found to be determined to a first approximation only by the shape of the face of the lithium block on which the flux is incident. Placing the sheets of steel closer together will result in a larger P_m, but will reduce the efficiency. For a square shape, the calculated P_m is 24%, and the measured P_m is 29 ± 2%. The lack of agreement is believed to be due to the collimation resulting from the lead shield in front of the scintillation detector.

The efficiency is defined as the flux entering the proportional counters divided by the incident flux. This has been found to be, to a first approximation,

$$E = \frac{1}{\alpha}\left[1 - e^{\alpha c}\right]\left[\frac{\chi_{ab}}{1 + k_{ab}\alpha} + \frac{\chi'_{ba}}{1 + k'_{ba}\alpha}\right] .$$

Lengths are measured in scattering lengths.

c = the length of the block measured in the direction of the incident flux.

a = the length of the side of the block through which the scattered flux enters the counters.

b = the length of the block along which there is a steel sheet.

α = total cross section/scattering cross section for absorption and scattering.

χ_{ab}, χ'_{ba}, k_{ab}, and k'_{ba} are wavelength-independent quantities which have been calculated for a number of values of the parameters. Measurements were made with the K_β line of molybdenum on a 5-3/8 x 2-1/2 x 2-1/2 inch lithium block. The calculated efficiency is 16.1%, and the measured efficiency was 13.5 ± 2%. The difference is believed to be due to a layer of oxide which formed on the lithium.

Measurements by Clark[1] indicate that we may expect a flux of 1/2 photons/cm^2/sec from the Crab nebula in the 15-50 keV range. With 300 seconds of observing time, we calculate that a polarization measurement of a few percent may be possible. The largest unknown factor is the number of background counts that will be recorded, and the extent to which these can be rejected by pulse height discrimination and rejection events which trigger more than one counter. Better estimates of the background rate can be made after measurements have been made on a prototype counter.

Program for the next interval: A prototype detector will be made of the above design.

(1) E. W. Clark, Phys. Rev. Letters 14, 91 (1965).

PERSONNEL

FACULTY

Professor R. Novick, Director	Optical Orientation of Atoms
Professor H. Boorse	Cryogenics
Professor P. Cahill	Molecular and Atomic Beam Physics
Professor S. Devons	Nuclear Polarization
Professor R. L. Disch	Molecular Physics
Professor H. M. Foley	Theoretical Physics
Professor S. R. Hartmann	Solid State Physics
Professor P. Kusch	Molecular and Atomic Beam Physics
Professor J. M. Luttinger	Theoretical Solid State Physics
Professor I. I. Rabi	Atomic Beams
Professor P. Thaddeus	Astrophysics

RESEARCH ASSOCIATES AND PHYSICISTS

Dr. I. D. Abella	Dr. P. Feldman	Dr. E. P. Jones
Dr. S. S. Alpert	Dr. L. P. Gold	Dr. W. W. Smith
M. J. Bernstein	Dr. W. Happer	Dr. Y. Yeh
Dr. L. M. Blau	Dr. R. C. Isler	Dr. S. Zemon
Dr. P. Davidovits	Dr. A. N. Jette	

GUEST RESEARCH STAFF

Dr. A. Lurio, Physicist, IBM Watson Laboratory

Dr. L. R. Wilcox, Associate Professor, American University of Beirut, Beirut, Lebanon

GRADUATE STUDENT RESEARCH ASSISTANTS

M. Dakss
S. Dworetsky
H. Einbinder
S. Fisher
S. Golub
D. Grischkowsky
M. M. Hessel
W. Ho
I. Kaufmann
F. Kantor
A. T-M. Kung
N. A. Kurnit
M. Levitt
M. Lipeles
T. Lucatorto
S. Marcus
R. Marzke
G. R. Mather
J. Matuska
B. Palatnick
D. Raskin
E. B. Saloman
L. Seigel
S. Skwire
G. Sprott
W. A. Stern
D. Sverdlik
M. Swagel
N. Tolk
T. E. Wing

TECHNICAL RESEARCH ASSISTANTS

I. Beller
C. U. Brown
J. Gorham
A. Lynch
W. Alexander
D. Balzarini
W. Conway
J. Werntz

ELECTRONICS SHOP

V. Foti
B. Rayhrer
A. Capriglione
F. Motika
M. Wizenberg

MACHINE SHOP

C. Dechert
W. Bauer
A. Filter
J. Haas
B. Hansen
E. Jauch
J. Robertson
M. Rossi

ADMINISTRATION

G. Castle
J. Ladue
E. LaForge
A. Lopez
E. Nesbitt

TECHNICAL EDITOR

V. M. Bennett

JOINT SERVICES DISTRIBUTION

DEPARTMENT OF DEFENSE

Dr. Chalmers Sherwin
Deputy Director
(Research & Technology)
DD & RE Rm 3E1060
The Pentagon
Washington, D. C. 20301

Dr. Edward M. Reilley
Asst. Director (Research)
Ofc of Defense Res & Eng
Department of Defense
Washington, D. C. 20301

Dr. James A. Ward
Office of Deputy Director
(Research and Information)
Rm 3D1037
Department of Defense
The Pentagon
Washington, D. C. 20301

Director
Advanced Research Projects Agency
Department of Defense
Washington, D. C. 20301

Professor Robb M. Thomson
Director for Materials Sciences
Room 3D 156
Advanced Research Projects Agency
Washington, D. C. 20301

Colonel Charles C. Mack
Defense Communications Agency
Attn: Code 333
Washington, D. C. 20305

20-Defense Documentation Center
Attn: TISIA
Cameron Station, Bldg. 5
Alexandria, Virginia 22314

Director
National Security Agency
Attn: Librarian C-332
Fort George G. Meade, Maryland
20755

DEPARTMENT OF THE ARMY

Chief of Research and Development
Headquarters, Department of
the Army
Attn: Mr. L. H. Geiger, Rm 3D442
Washington, D. C. 20310

Chief of Research and Development
Attn: Physical Sciences Division
Department of the Army
Washington, D. C. 20310

Research Plans Office
U. S. Army Research Office
3045 Columbia Pike
Arlington, Virginia 22204

Commanding Officer
U. S. Army Foreign Science
and Technology Center
Attn: AMXST-SD-TD
Washington, D. C. 20315

Commanding General
U. S. Army Materiel Command
Attn: AMCRD-RS-PE-E
Washington, D. C. 20315

Commanding General
U. S. Army Strategic
Communications Command
Washington, D. C. 20315

Commanding Officer
U. S. Army Materials Research
Agency
Watertown Arsenal
Watertown, Massachusetts 02172

Commanding Officer
U. S. Army Ballistics Research
Laboratory
Attn: V. W. Richards
Aberdeen Proving Ground
Aberdeen, Maryland 21005

DEPARTMENT OF THE ARMY (cont)

Commanding Officer
U. S. Army Ballistics Research
Laboratory
Attn: Keats A. Pullen, Jr.
Aberdeen Proving Ground
Aberdeen, Maryland 21005

Commanding Officer
U. S. Army Ballistics Research
Laboratory
Attn: George C. Francis,
Computing Lab
Aberdeen Proving Ground
Aberdeen, Maryland 21005

Commandant
U. S. Army Air Defense School
Attn: Missile Science Division
C&S Department
P. O. Box 9390
Fort Bliss, Texas 79916

Commanding General
U. S. Army Missile Command
Attn: Technical Library
Redstone Arsenal, Alabama 35809

Commanding Officer
Frankford Arsenal
Attn: Pitman-Dunn Research Lab
SMUFA-L1000-64-4
Philadelphia, Pa. 19137

U. S. Army Munitions Command
Attn: Technical Information
Branch
Picatinney Arsenal
Dover, New Jersey 07801

Commanding Officer
Harry Diamond Laboratories
Attn: Mr. Berthold Altman
Connecticut Ave. &
Van Ness St. N. W.
Washington, D. C. 20438

Commanding Officer
Harry Diamond Laboratories
Attn: Library
Connecticut Ave. &
Van Ness St., N. W.
Washington, D. C. 20438

Commanding Officer
Harry Diamond Laboratories
Attn: Dr. R. T. Young
Electron Tubes Division
Connecticut Ave. &
Van Ness St., N. W.
Washington, D. C. 20438

Commanding Officer
U. S. Army Security Agency
Arlington Hall
Arlington, Virginia 22212

Commanding Officer
U. S. A. Limited War Laboratory
Attn: Technical Director
Aberdeen Proving Ground
Aberdeen, Maryland 21005

Commanding Officer
Human Engineering Laboratories
Aberdeen Proving Ground
Aberdeen, Maryland 21005

Director
U. S. Army Engineer Goedesy
Intelligence and Mapping
Research and Development Agency
Attn: ENGGM-RA (Mr. J. F. Hannigan)
Fort Belvoir, Virginia 22060

Commandant
U. S. Army Command and General
Staff College
Attn: Acquisitions, Library
Division
Fort Leavenworth, Kansas 66207

Dr. H. Robl
Deputy Chief Scientist
U. S. Army Research Office (Durham)
Box CM, Duke Station
Durham, North Carolina 27706

DEPARTMENT OF THE ARMY (cont)

Commanding Officer
U. S. Army Research Office
(Durham)
Attn: CRD-AA-IP
(Richard O. Ulsh)
P. O. Box CM, Duke Station
Durham, North Carolina 27706

Dr. S. Benedict Levin, Director
Institute for Exploratory Research
U. S. Army Electronics Command
Fort Monmouth, New Jersey 07703

Director
Institute for Exploratory Research
U. S. Army Electronics Command
Attn: Mr. Robert O. Parker,
Executive Secretary
JSTAC (AMSEL-XL-D)
Fort Monmouth, New Jersey 07703

Superintendent
U. S. Army Military Academy
West Point, New York 10996

Division of Nuclear Medicine
Walter Reed Army Institute of
Research
Walter Reed Army Medical Center
Washington, D. C. 20012

Commanding Officer
U. S. Army Engineers
R & D Laboratory
Attn: STINFO Branch
Fort Belvoir, Virginia 22060

Mr. A. D. Bedrosian
Room 26-131
USAECOM Scientific LnO
Mass. Institute of Technology
77 Massachusetts Ave.
Cambridge, Massachusetts 02139

Commanding Officer
U. S. Army Electronics R & D
Activity, Arizona
Attn: SELHU-PT
Fort Huachuca, Arizona 85613

Commanding Officer
U. S. Army Electronics
R & D Activity
White Sands Missile Range
New Mexico 88002

Commanding General
U. S. Army Electronics
Proving Ground
Attn: Technical Library, LN-403
Fort Huachuca, Arizona 85613

Director
Human Resources Research Office
The George Washington University
300 N. Washington Street
Alexandria, Virginia

Commanding Officer
U. S. Army Personnel Research
Office
Washington 25, D. C.

Commanding Officer
U. S. Army Medical Research
Laboratory
Attn: Biophysics Division
Fort Knox, Kentucky 40121

Commanding General
U. S. Army Electronics Command
Fort Monmouth, New Jersey 07703
(1) to each symbol
Attn: AMSEL-

XL-D	NL-S	NL-P
XL-E	KL-D	NL-R
XL-C	KL-E	RD-GF
XL-S	KL-SM	RD-MN
HL-D	KL-T	(Marine
HL-L	VL-D	Corps LnO)
HL-J	WL-D	
HL-P	SC	
HL-O	RD-D	
HL-R	RD-G	
NL-D	RD-MAF-1	
NL-A	RD-MAT	

Note: One (1) copy to each addressee unless otherwise indicated

DEPARTMENT OF THE NAVY

Dr. Arnold Shostak, Code 427
Head, Electronics Branch
Physical Sciences Division
Department of the Navy
Office of Naval Research
Washington, D. C. 20360

2-Chief of Naval Research
Code 427
Department of the Navy
Washington, D. C. 20360

Chief, Bureau of Weapons
Department of the Navy
Washington, D. C. 20360

Chief, Bureau of Ships
Department of the Navy
Washington, D. C. 20360
Attn: Code 680

Commander
U. S. Naval Air Development Center
Johnsville, Pennsylvania
Attn: NADC Library

Commanding Officer
Naval Electronics Laboratory
San Diego, California
Attn: Code 2222

Commander
Naval Ordnance Laboratory
White Oak, Maryland 20910
Attn: Technical Library

U. S. Navy Post Graduate School
Monterrey, California
Attn: Electrical Engineering Department

Commanding Officer
U. S. Navy Underwater Sound Laboratory
Fort Trumbull
New London, Connecticut

6-Director
Naval Research Laboratory
Washington, D. C. 20390

Commanding Officer
Office of Naval Research
Branch Office
Navy 100, Fleet P.O. Box 39
New York, N. Y.

Chief of Naval Operations
Pentagon OP 07T
Washington, D. C.

Commanding Officer
Office of Naval Research
Branch Office
207 West 24th Street
New York, N. Y. 10011

DEPARTMENT OF THE AIR FORCE

5-Lt. Col. Edmund P. Gaines, Jr. SREE
Chief, Electronics Division
Directorate of Engineering Sciences
Air Force Office of Scientific Research
Washington, D. C. 20333

Honorable Alexander H. Flax
Asst Secretary of the Air Force (R & D)
Office of the Secretary of the Air Force
Washington, D. C. 20301

Colonel J. T. Stewart
Director of Science & Technology
Deputy Chief of Staff (R & D)
USAF
Washington, D. C. 20301

3-Commander
Air Force Office of Scientific Research
Attn: SRPP
Washington, D. C. 20333

DEPARTMENT OF THE AIR FORCE (cont)

Karl M. Fuechsel
Electronics Division
Directorate of Engineering Sciences
Air Force Office of Scientific Research
Washington, D. C. 20333

Maj. John M. MacCallum, Jr.
Headquarters, USAF (AFRSTE)
Washington 25, D. C.

Air Force Office of Scientific Research
Attn: SRMA
Washington, D. C. 20333

Air Force Office of Scientific Research
Attn: SRY
Washington, D. C. 20333

Commander
Air Force Research Division
Attn: RRRTL
Washington 25, D. C.

Director of Research and Development
Headquarters USAF
Attn: AFRDR
Washington 25, D. C.

Commander
Wright Air Development Center
Wright-Patterson AFB
Ohio 45433
Attn: WWAD

Director
Air University Library
Maxwell Air Force Base
Alabama 36112

Headquarters RTD (RTTC)
Bolling AFB
Washington, D. C.

Commander
Air Force Cambridge Research Laboratories
Office of the Scientific Director
L. G. Hanscom Field
Bedford, Massachusetts 01731

Dr. Lowell M. Hollingsworth
Technical Advisor for Electronics
AFCRL(CRN)
L. G. Hanscom Field
Bedford, Massachusetts 01731

Commander
Air Force Cambridge Research Laboratories
Attn: CRREL
L. G. Hanscom Field
Bedford, Massachusetts 01731

ESD (ESTI)
L. G. Hanscom Field
Bedford, Massachusetts 01731

Space Systems Division
Los Angeles Air Force Station
Los Angeles, California 90045
Attn: SSSD

AFETR Technical Library
(ETV-MU-135)
Patrick AFB, Florida 32925

Commander
Air Force Systems Command
Office of the Chief Scientist
Andrews AFB, Maryland 20331

Commander
Air Force Missile Development Center
Attn: HD01
Holloman Air Force Base
New Mexico

DEPARTMENT OF THE AIR FORCE (cont)

Commander
Air Force Special Weapons Center
Attn: SW01
Kirtland Air Force Base
New Mexico 87117

Sandia Corporation
P. O. Box 5800
Sandia Base
Albuquerque, New Mexico 87115
Attn: Technical Library

AFSC Scientific and Technical Liaison Office
Research and Technology Division
111 East 16th Street
New York, N. Y. 10003
Attn: Mr. Morton M. Pavane, Chief

Arnold Air Force Station
AEDC (AEOIM)
Attn: Technical Library
Tullahoma, Tennessee

ASD (ASGS)
Wright-Patterson AFB
Ohio 45433

Systems Engineering Group (RTD)
Attn: SEPIR
Wright-Patterson AFB
Ohio 45433

Commandant
Air Force Institute of Technology
(AU) Library MCLI-LIB
Bldg 125, Area B
Wright-Patterson AFB
Ohio 45433

AFAL(AVTE)
Wright-Patterson AFB
Ohio 45433

Aeronautical Research Laboratories
Attn: Technical Library
Bldg 450
Wright-Patterson AFB
Ohio 45433

Headquarters
Aeronautical Systems Division
AF Systems Command
Attn: George R. Branner
ASSRNEA-2
Wright-Patterson AFB
Ohio 45433

Aerospace Research Laboratories (ARIY)
Wright-Patterson AFB
Ohio 45433

Office of the Chief Scientist
Chief of Staff, USAF
Washington, D. C.

Headquarters
Aeronautical Systems Division
Attn: ASRNET-3
Wright-Patterson AFB
Ohio 45433

Commander
Rome Air Development Center
Attn: EMLAL-1
Griffiss Air Force Base
Rome, New York 13442

DEPARTMENT OF COMMERCE

2-National Bureau of Standards
Boulder, Colorado 80301
Attn: Radio Standards Physics Division, 251.00

Library
National Bureau of Standards
Boulder Laboratories
Boulder, Colorado 80301

Clearinghouse
5285 Port Royal Road
Springfield, Virginia 22151

OTHER GOVERNMENT AGENCIES

Mr. Charles F. Yost
Special Assistant to the
Director of Research
National Aeronautics and
Space Administration
Washington, D. C. 20546

U. S. Atomic Energy Commission
1901 Constitution Avenue, N. W.
Washington 25, D. C.

Manager Operations
U. S. Atomic Energy Commission
180 Varick Street
New York, N. Y. 10014
Attn: Library Section

4-U. S. Atomic Energy Commission
P. O. Box E
Oak Ridge, Tennessee
Attn: Technical Information
Division, ORE

Dr. F. O. Vonbun, Chief
Mission Analysis Office
Code 507
NASA Goddard Space Flight Center
Greenbelt, Maryland

National Aeronautics and Space
Administration
Office of Advanced Research
Technology
1512 H Street, N. W.
Washington 25, D. C.
Attn: Dr. H. Harrison, Code RRE

Headquarters
National Aeronautics and Space
Administration
400 Maryland Avenue, S. W.
Washington 25, D. C.
Attn: Office of Applications
Code FC

3-National Aeronautics and Space
Administration
Washington 25, D. C.
Attn: Office of Research Grants
and Contracts Code: SC

Scientific and Technical
Information Facility
P. O. Box 5700
Bethesda, Maryland
Attn: NASA Representatives
(S-AK/DL)

NON-GOVERNMENT LIST

British Joint Services Mission
(Navy Staff)
P. O. Box 165
Benjamin Franklin Station
Washington 6, D. C.
Attn: Mr. F. H. Powell

Canadian Joint Staff
2450 Massachusetts Ave., N. W.
Washington, D. C. 20008
Attn: Defense Research Member

General Dynamics/Astronautics
P. O. Box 1128
San Diego 12, California
Attn: Dr. D. H. Garber
Mail Zone 595-4

Engineering Library
ITT Gilfillan Inc.
1815 Venice Blvd.
Los Angeles, California 90006

Hughes Research Laboratory
P. O. Box 338
Malibu, California

Institute for Defense Analyses
Communications Research Division
Von Neumann Hall
Princeton, New Jersey

NON-GOVERNMENT LIST (cont)

Carlyle Barton Laboratory
The Johns Hopkins University
Charles and 34th Sts.
Baltimore, Maryland 21218
Attn: Librarian

The Johns Hopkins University
Applied Physics Laboratory
8621 Georgia Avenue
Silver Spring, Maryland

The Martin Company
Post Office Box 5837
Orlando, Florida
Attn: The Library, Mail MP-30

Director
Research Laboratory of Electronics
Mass. Institute of Technology
Cambridge, Massachusetts 02139

Massachusetts Institute of
Technology
Lincoln Laboratory
Lexington 73, Massachusetts
Attn: Dr. J. W. Meyer

Microwave Associates, Inc.
South Avenue
Burlington, Massachusetts

NASA-ERC
575 Technology Square
Cambridge, Massachusetts 02139
Attn: Dr. Norman Knable
Space Optics Laboratory

National Science Foundation
Washington 25, D. C.
Attn: Director

The Ohio State University
Antenna Laboratory
1320 Kinnear Road
Columbus, Ohio 43212

Director of Engineering and
Applied Physics
210 Pierce Hall
Harvard University
Cambridge, Massachusetts 02138

Brandeis University
Department of Physics
Waltham, Massachusetts 02154
Attn: Prof. E. Lipworth

Mr. Jerome Fox
Research Coordinator
Polytechnic Institute of Brooklyn
333 Jay Street
Brooklyn, New York 11201

Raytheon Company
28 Seyon Street
Waltham, Massachusetts 02154
Attn: Research Division
Laboratory

Director
Coordinated Science Laboratories
University of Illinois
Urbana, Illinois

Stanford University
Division of Applied Physics
McCullough Building
Stanford, California
Attn: H. Heffner

Stanford University
Microwave Laboratory
W. W. Hansen Laboratories
of Physics
Stanford, California
Attn: Librarian

Solid-State Electronics
Laboratory
Stanford University
Stanford, California
Attn: Prof. J. B. Angell

NON-GOVERNMENT LIST (cont)

Sylvania Electric Products, Inc.
100 Sylvan Road
Woburn, Massachusetts
Attn: Semiconductor Division
Library

University of California
Department of Engineering
Berkeley 4, California
1-Attn: Professor J. R. Singer
Division of Electrical
Engineering
1-Attn: Electronics Research
Laboratory

University of Southern California
Technical Report Librarian
Olin Hall of Engineering
Electronic Sciences Laboratory
Los Angeles, California 90007

University of Southern California
Los Angeles, California 90007
Attn: Electronic Sciences
Laboratory

2-University of Colorado
Research Service Laboratories
Boulder, Colorado
Attn: Technical Coordinator

University of Michigan
Institute of Science and
Technology
P. O. Box 618
Ann Arbor, Michigan
Attn: IRIA

The University of Texas
Department of Electrical
Engineering
Engineering Science Bldg. 112
Austin, Texas 78712
Attn: Prof. A. A. Dougal

The University of Michigan
Institute of Science and
Technology
Attn: Technical Documents Service
Box 618
Ann Arbor, Michigan 48107

The University of Michigan
Cooley Electronics Laboratory
Room 262, Cooley Building
North Campus
Ann Arbor, Michigan
Attn: Dr. Thomas W. Butler, Jr.
Director

Prof. A. A. Dougal, Director
Laboratory for Electronics and
Related Science Research
University of Texas
Austin, Texas 78712

University of Utah
Microwave Devices Laboratory
Salt Lake City, Utah 84112
Attn: Dr. R. W. Grow

FOREIGN LIST

(Copies are transmitted via:
Office of Foreign Programs
Office of Defense Research
and Engineering
Pentagon Building
Washington 25, D. C.
Attn: F. D. Hege)

Commonwealth Scientific and
Industrial Research Organization
National Standards Laboratory
University Grounds, City Road
Chippendale, N.S.W., Australia
Attn: F. J. Lehany, Chief
Division of Applied Physics

National Research Council
Sussex Drive
Ottawa 2, Canada
Attn: G. Herzberg, Director
Division of Pure Physics

FOREIGN LIST (cont)

The British Thomson-Houston
Co., Ltd.
Rugby, Warwickshire, England
Attn: Dr. R. Dunsmuir,
Research Laboratory

Central Electricity Research
Laboratories
Kingston Road
Leatherhead, Surrey, England
Attn: Dr. Peter Chester
Solid-State Physics Section

The Clarendon Laboratory
Parks Road
Oxford, England
Attn: Dr. B. Bleaney

Department of Electrical
Engineering
University of Newcastle
upon Tyne
Merz Laboratories
Newcastle upon Tyne, 1
England

Ministry of Aviation
Royal Radar Establishment
Malvern, Worchestershire, England
Attn: Dr. R. A. Smith
Physics Department

Mullard Research Laboratories
Redhill, Surrey
England
Attn: Dr. J. C. Walling

Services Electronics
Research Laboratory
Baldock, Herts, England

Central Electronics Engineering
Research Institute
Pilani, Rajasthan, India
Attn: Om P. Gandhi
Assistant Director

Mrs. Brita Nachmanson
Acquisition Librarian
Royal Institute of Technology
Library
Stockholm 70. Sweden

The Librarian
University of Otago
Dunedin, New Zealand

Saha Institute of Nuclear Physics
92 Acharya Prafulla, Chandra Road
Calcutta 9, India
Attn: P. Hosain, Librarian

Security Classification

DOCUMENT CONTROL DATA · R&D

(Security classification of title, body of abstract and indexing annotation must be entered when the overall report is classified)

1. ORIGINATING ACTIVITY (Corporate author) COLUMBIA UNIVERSITY, Dep't of Physics Columbia Radiation Laboratory New York, N. Y. 10027	2a. REPORT SECURITY CLASSIFICATION Unclassified 2b. GROUP

3. REPORT TITLE

RESEARCH INVESTIGATION DIRECTED TOWARD EXTENDING THE USEFUL RANGE OF THE ELECTROMAGNETIC SPECTRUM

4. DESCRIPTIVE NOTES (Type of report and inclusive dates)

Quarterly Progress Report, 16 June 65 - 15 September 65

5. AUTHOR(S) (Last name, first name, initial)

Novick, Robert : Director CRL

6. REPORT DATE	7a. TOTAL NO. OF PAGES	7b. NO. OF REFS
15 September 1965	vi + 73	46

8a. CONTRACT OR GRANT NO.	9a. ORIGINATOR'S REPORT NUMBER(S)
DA-28-043 AMC-00099(E) b. PROJECT NO. DA-1A0-10501-B010 c. d.	Progress Report No. 11 9b. OTHER REPORT NO(S) (Any other numbers that may be assigned this report) CU-9-65 AMC-00099(E) Physics

10. AVAILABILITY/LIMITATION NOTICES

Qualified requestors may obtain copies of this report from DDC.

11. SUPPLEMENTARY NOTES	12. SPONSORING MILITARY ACTIVITY
	Joint Services Electronics Program (Army, Navy, Air Force)

13. ABSTRACT

Recent work has shown that under many experimental conditions, the decay of an ensemble of excited atoms is characterized by several relaxation times. Physically, these are the lifetime of the population of excited atoms, the lifetime of the average magnetic dipole moment (or orientation), the lifetime of the average electric quadrupole moment (or alignment), and the lifetimes of higher atomic multipole moments. Each multipole moment of the excited atoms decays with a characteristic lifetime because of the isotropy of the surrounding medium. In the limit of low vapor pressure, all of these lifetimes reduce to the natural radiative lifetime of the atom. In level-crossing experiments one can measure the lifetime of orientation and alignment separately. This is in contrast to classical nuclear magnetic resonance experiments, where only one parameter can be measured. The added flexibility in level-crossing experiments arises from the possibility of measuring the polarization of the fluorescent light. The existence of two lifetimes has been observed in Hanle-effect signals from the first $^3P_1{}^\circ$ state in lead when the signal was subject to resonant self-broadening, and also in the presence of foreign gas broadening and coherence narrowing.

DD FORM 1 JAN 64 1473

Unclassified

Security Classification

14. KEY WORDS	LINK A		LINK B		LINK C	
	ROLE	WT	ROLE	WT	ROLE	WT
Two-photon decay of singly ionized helium Optical excitation with low-energy ions Level-crossing experiments Rf spectroscopy; He^- ion Hyperfine structure of Group IIA isotopes Fine and Hyperfine structure of the 3P state of Li^7 Optical studies of atoms Molecular spectroscopy; Solid state Optical maser spectroscopy Molecular birefringence Photon-echo resonance in ruby; Rubidium maser; Models of planetary atmospheres Polarization measurements						

INSTRUCTIONS

1. ORIGINATING ACTIVITY: Enter the name and address of the contractor, subcontractor, grantee, Department of Defense activity or other organization *(corporate author)* issuing the report.

2a. REPORT SECURITY CLASSIFICATION: Enter the overall security classification of the report. Indicate whether "Restricted Data" is included. Marking is to be in accordance with appropriate security regulations.

2b. GROUP: Automatic downgrading is specified in DoD Directive 5200.10 and Armed Forces Industrial Manual. Enter the group number. Also, when applicable, show that optional markings have been used for Group 3 and Group 4 as authorized.

3. REPORT TITLE: Enter the complete report title in all capital letters. Titles in all cases should be unclassified. If a meaningful title cannot be selected without classification, show title classification in all capitals in parenthesis immediately following the title.

4. DESCRIPTIVE NOTES: If appropriate, enter the type of report, e.g., interim, progress, summary, annual, or final. Give the inclusive dates when a specific reporting period is covered.

5. AUTHOR(S): Enter the name(s) of author(s) as shown on or in the report. Enter last name, first name, middle initial. If military, show rank and branch of service. The name of the principal author is an absolute minimum requirement.

6. REPORT DATE: Enter the date of the report as day, month, year; or month, year. If more than one date appears on the report, use date of publication.

7a. TOTAL NUMBER OF PAGES: The total page count should follow normal pagination procedures, i.e., enter the number of pages containing information.

7b. NUMBER OF REFERENCES: Enter the total number of references cited in the report.

8a. CONTRACT OR GRANT NUMBER: If appropriate, enter the applicable number of the contract or grant under which the report was written.

8b, 8c, & 8d. PROJECT NUMBER: Enter the appropriate military department identification, such as project number, subproject number, system numbers, task number, etc.

9a. ORIGINATOR'S REPORT NUMBER(S): Enter the official report number by which the document will be identified and controlled by the originating activity. This number must be unique to this report.

9b. OTHER REPORT NUMBER(S): If the report has been assigned any other report numbers *(either by the originator or by the sponsor)*, also enter this number(s).

10. AVAILABILITY/LIMITATION NOTICES: Enter any limitations on further dissemination of the report, other than those imposed by security classification, using standard statements such as:

(1) "Qualified requesters may obtain copies of this report from DDC."

(2) "Foreign announcement and dissemination of this report by DDC is not authorized."

(3) "U. S. Government agencies may obtain copies of this report directly from DDC. Other qualified DDC users shall request through

_____."

(4) "U. S. military agencies may obtain copies of this report directly from DDC. Other qualified users shall request through

_____."

(5) "All distribution of this report is controlled. Qualified DDC users shall request through

_____."

If the report has been furnished to the Office of Technical Services, Department of Commerce, for sale to the public, indicate this fact and enter the price, if known.

11. SUPPLEMENTARY NOTES: Use for additional explanatory notes.

12. SPONSORING MILITARY ACTIVITY: Enter the name of the departmental project office or laboratory sponsoring *(paying for)* the research and development. Include address.

13. ABSTRACT: Enter an abstract giving a brief and factual summary of the document indicative of the report, even though it may also appear elsewhere in the body of the technical report. If additional space is required, a continuation sheet shall be attached.

It is highly desirable that the abstract of classified reports be unclassified. Each paragraph of the abstract shall end with an indication of the military security classification of the information in the paragraph, represented as *(TS), (S), (C), or (U)*.

There is no limitation on the length of the abstract. However, the suggested length is from 150 to 225 words.

14. KEY WORDS: Key words are technically meaningful terms or short phrases that characterize a report and may be used as index entries for cataloging the report. Key words must be selected so that no security classification is required. Identifiers, such as equipment model designation, trade name, military project code name, geographic location, may be used as key words but will be followed by an indication of technical context. The assignment of links, rules, and weights is optional.

13. ABSTRACT (cont'd)

Radiation due to the impact of very slow helium ions on the rare gases has been observed. The dependence of the cross section on the kinetic energy of the He^+ beam shows unexpected and important features down to the lowest energies studied (5 eV). The absolute cross sections are typically of the order of 10^{-16} cm^2 and in some cases are almost an order of magnitude larger. In at least one case, the radiation has been shown to result from charge exchange with simultaneous excitation.

Systematic observations have been made on the spectra of 6328Å light scattered from carbon dioxide near the critical temperature T_c and the critical density ρ_c. These studies were made as a function of both scattering angle θ and temperature T using an f/7 collecting lens. A new optical system has been developed which uses a lensless geometry and is capable of defining scattering angles to an accuracy better than ± 10' of arc without any averaging effects of a collecting lens.